DIABETES RESEARCH AND CLINICAL PRACTICE 80 (2008) e16–e19

available at www.sciencedirect.com

ScienceDirect

journal homepage: www.elsevier.com/locate/diabres

Brief report

Short-term intensive glycemic control improves vibratory sensation in type 2 diabetes

Yoshihito Fujita [a], Mitsuo Fukushima [a,b,*], Haruhiko Suzuki [a], Ataru Taniguchi [c], Yoshikatsu Nakai [d], Akira Kuroe [c], Koichiro Yasuda [a], Masaya Hosokawa [a], Yuichiro Yamada [a], Nobuya Inagaki [a], Yutaka Seino [a,c]

[a] Department of Diabetes and Clinical Nutrition, Graduate School of Medicine, Kyoto University, 54 Shogoin-Kawahara-cho, Sakyo-ku, Kyoto 606-8507, Japan
[b] Foundation for Biomedical Research and Innovation, Translational Research Informatics Center, Hyogo, Japan
[c] Kansai-Denryoku Hospital, Osaka, Japan
[d] College of Medical Technology, Kyoto University, Kyoto, Japan

ARTICLE INFO

Article history:
Received 22 November 2007
Accepted 12 December 2007
Published on line 8 February 2008

Keywords:
Vibratory sensation
Diabetic peripheral neuropathy
Glycemic control
Glucose metabolism
Lipid metabolism

ABSTRACT

Strict long-term glycemic control has been reported to prevent or improve diabetic peripheral neuropathy, but the effects of short-term glycemic control have not been clarified in patients with type 2 diabetes. To investigate reversibility of impaired vibratory sensation by short-term glycemic control, we used the TM31 liminometer and C64 tuning fork methods to measure peripheral neuropathy. Thirty-one type 2 diabetes patients with poor glycemic control (HbA1c: 10.8 ± 0.4%, mean ± S.E.M., range from 7.9% to 16.2%) were administered strict glycemic control. Vibratory sensation before and after short-term glycemic control was evaluated, and the metabolic profile including plasma glucose, HbA1c, total cholesterol, HDL cholesterol, triglyceride, and free fatty acid (FFA) was measured. After 20.0 ± 2.1 days of strict glycemic control, vibratory sensation improved significantly in both upper and lower extremities, assessed by TM31 liminometer and C64 tuning fork. Along with the improved glycemic control, lipid metabolism (total cholesterol, triglyceride and FFA) was significantly improved. Thus, short-term intensive glycemic control can improve vibratory sensation, metabolic changes in glucose and lipid metabolism being the factors responsible for improved of peripheral nerve function.

1. Introduction

Strict glycemic control can improve diabetic peripheral neuropathy in patients with type 1 diabetes [1,2], and preserve it in patients with type 2 diabetes [3,4]. In addition, there is some evidence that both long- and short-term glycemic control can improve vibratory sensation in patients with type 1 diabetes [5]. However, there are few reports regarding short-term glycemic control and vibratory sensation in patients with type 2 diabetes, in whom clinical development of the disease and its complications is more slowly progressive. In this study, we compared vibratory sensation before and after rigorous

* *Corresponding author at*: Department of Diabetes and Clinical Nutrition, Graduate School of Medicine, Kyoto University, 54 Kawahara-cho, Shogoin, Sakyo-ku, Kyoto 606-8507, Japan. Tel.: +81 75 751 3560; fax: +81 75 751 4244.
E-mail address: fukum@tri-kobe.org (M. Fukushima).
0168-8227/$ – see front matter © 2008 Published by Elsevier Ireland Ltd.
doi:10.1016/j.diabres.2007.12.011

short-term glycemic control in Japanese type 2 diabetes patients. We used the TM31 liminometer and the C64 tuning fork methods to evaluate vibratory sensation [6–9]. Metabolic profiles were also examined before and after short-term glycemic control to clarify the factors involved in the restoration of vibratory sensation.

2. Patients and methods

Thirty-one type 2 diabetes patients who had poor glycemic control on admission to Kyoto University Hospital during June 2002 and January 2004 were administered strict glycemic control by intensive insulin therapy and diet. The patients were 20–70 of age, and those with other neurological disorders that can cause peripheral neuropathy such as familial, alcoholic, uremic or endocrine neuropathy were excluded. The threshold of vibratory sensation and plasma glucose, total cholesterol, HDL cholesterol, triglyceride and free fatty acid (FFA) were compared on admission and before discharge.

The clinical characteristics at admission were as follows. Duration of diabetes was 9.4 ± 1.7 years. Of 31 patients, 20 were male and 11 were female. The average age and BMI were 59.0 ± 2.2 years and 24.6 ± 0.8 kg/m^2, respectively. HbA1c was $10.8 \pm 0.4\%$, mean $\pm$ S.E.M., ranging from 7.9% to 16.2%. Fifteen patients had diabetic retinopathy and 3 had diabetic nephropathy with proteinuria. None of the patients had painful neuropathy, but 10 patients had abnormality of deep reflex testing (ankle reflex and/or knee reflex) for both lower limbs. The threshold of vibratory sensation was evaluated by two separate tests. The TM31 liminometer (Medic International Co. Ltd., Tokyo, Japan) measurements of vibratory sensation were performed at the radial malleoli of both hands and the medial malleoli of both feet [4,8,9]. The amplitude was increased and decreased from 0 μm to 155 μm at a constant rate to ascertain the threshold of vibratory sensation. C64 quantitative tuning fork (Takano Manufacturing Co., Nagoya, Japan) measurements, which quantify the severity of deficits in vibratory sensation on a scale of 0 (minimum score) to 8 (maximum score), were performed at the radial malleoli of both hands and the medial malleoli of both feet and the first toe of both feet. Based on the results of previous studies, normal values up to 40 years should be at least 6/8, while patients older than 40 years should score at least 4/8 [6,7,10].

Each measurement was performed by the same examiner and done three times to calculate the mean. To evaluate the accuracy of the vibratory test, we preliminarily examined correlation of two methods in 157 patients. TM31 liminometer and C64 tuning fork measurements showed remarkably high correlation at both upper and lower extremities. As representative, left foot measurements are compared in Fig. 1(A) ($p < 0.001$, $r = 0.95$).

HbA1c was measured on admission and the following month. Plasma glucose, HbA1c, serum total cholesterol, HDL cholesterol, triglyceride and FFA concentration were measured as reported previously [11,12]. The study was designed in compliance with the ethics regulations set out by the Helsinki declaration.

Data are presented as means $\pm$ S.E.M. Statistical analyses were performed by STATVIEW 5 system (StatView, Berkeley, CA). Differences between the two groups were assessed by Student's *t*-test. Regression analysis also was performed to study the distribution. *p*-Values less than 0.05 were considered statistically significant.

3. Results

After 20.0 ± 2.1 days of strict glycemic control, vibratory sensation improved significantly in both upper and lower extremities as assessed by TM31 liminometer. Similar results were obtained by C64 tuning fork (Fig. 1(B)). Vibratory sensation improved at the medial malleus of the left foot as assessed by both TM31 liminometer ($p < 0.01$) and C64 tuning fork ($p < 0.001$).

Along with improved glycemic control (HbA1c reduced from $10.8 \pm 0.4\%$ to $9.0 \pm 0.3\%$ and fasting plasma glucose reduced from 209.8 ± 11.7 mg/dl to 116.2 ± 5.7 mg/dl), and lipid metabolism significantly improved. The total cholesterol concentration declined from 217.0 ± 7.0 mg/dl to 193.3 ± 7.3 mg/dl ($p < 0.001$), the triglyceride concentration declined from 155.8 ± 19.0 mg/dl to 115.6 ± 10.8 mg/dl ($p < 0.01$), and the FFA concentration declined from 733.9 ± 68.2 mequiv./dl to 581.6 ± 48.4 mequiv./dl ($p < 0.01$).

4. Discussion

The development of diabetic peripheral neuropathy has been considered irreversible [13]. However, it has been shown that long-term strict glycemic control can improve diabetic peripheral neuropathy in patients with type 1 diabetes [1,2] and preserve it in patients with type 2 diabetes [3,4]. In addition, it has recently been reported that spontaneous recovery from diabetes resulting in near-euglycemia allows many features of neuropathy to recover in murine diabetes models [14]. In the present study, improvement of vibratory sensation evaluated by the two different methods in upper and lower extremities after 20 days of strict glycemic control demonstrates that vibratory sensation in type 2 diabetic patients can be ameliorated by short-term glycemic control. In addition, when the 31 patients were divided into a good improvement and a little improvement group, the good improvement group showed reduction to $2.7 \pm 0.6\%$, while the little improvement group was reduced only to $1.6 \pm 0.3\%$. The difference may reflect a relationship between improved vibratory sensation and improved glycemic control.

Both TM31 liminometer and C64 quantitative tuning fork measurements were used in this study. Independent examinations were performed three times in each patient at three different places. The two measurements correlated well, indicating that sensitivity of the C64 tuning fork is comparable to that of the TM31 liminometer, and is useful clinically as a simple diagnostic tool [15,16].

The duration of diabetes averaged 9.4 ± 1.7 years, and many subjects had overt diabetic complications. Because the UKPDS study recruited newly diagnosed type 2 patients and treatment was for 10 years, it is possible that the effect on neuropathy was a consequence of long-term glycemic control since the beginning of early-stage diabetic neuropathy [3].

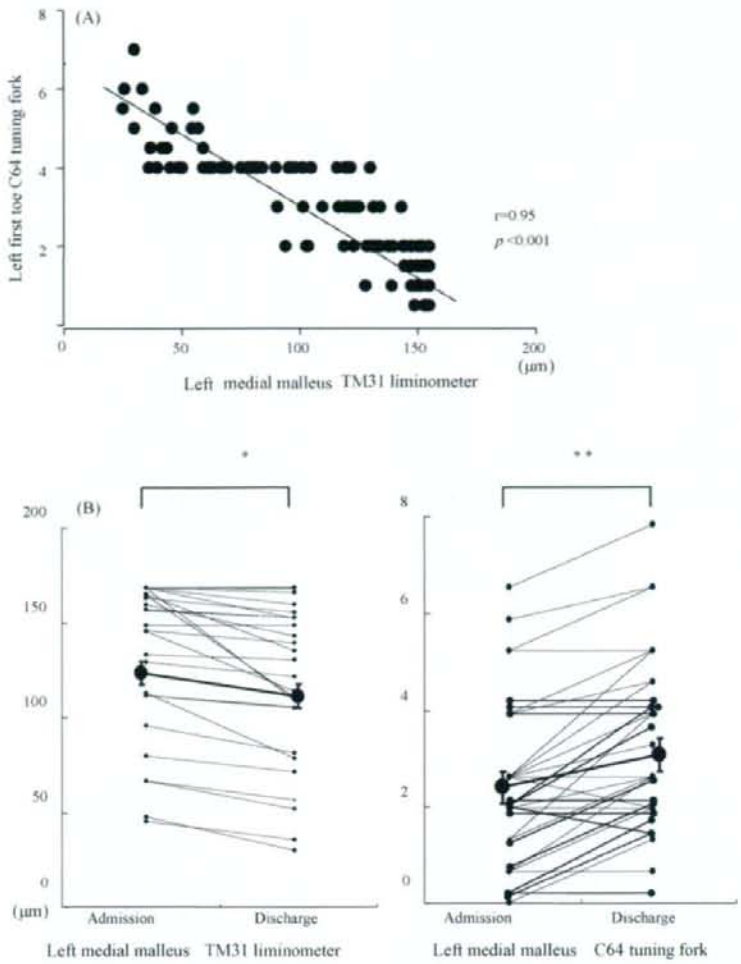

Fig. 1 – (A) Comparison of TM31 liminometer and C64 tuning fork measurements; (B) changes in vibratory sensation by short-term glycemic control. Closed circles and thick bars represent mean ± S.E.M. *$p < 0.01$, **$p < 0.001$.

Type 2 diabetes generally progresses slowly, and many patients already have diabetic polyneuropathy when they are diagnosed. We found that short-term glycemic control improved vibratory sensation even in patients with progressive diabetic polyneuropathy, and the DCCT study reported improved nerve conduction velocity and CVR-R during long-term intensive glycemic control. Thus, improvement of neurological function, at least in type 1 diabetes, might well follow systemic change derived from intensive glycemic control. Further studies are required to determine if autonomic function also can be improved during short-term intensive glycemic control in patients with type 2 diabetes.

Long-term studies such as UKPDS covered over 10 years, while the measurement interval of our study was only 20.0 ± 2.1 days. The factors known to be involved in improvement by long-term control are histological changes, typically related to decreased myelinated fiber density or loss of nerve fibers with axonal degeneration of remaining fibers [17,18]. By contrast, metabolic changes are probably responsible for improvement by short-term control. Lipid metabolism as well as glucose metabolism was found to be improved by short-term hospitalization. It has been reported that higher triglyceride concentrations are correlated with polyneuropathy [19], so improvement of lipid metabolism also may contribute to improved vibratory sensation.

In conclusion, we have shown that short-term intensive glycemic control can improve vibratory sensation that can be detected by C64 tuning fork as well as by TM31 liminometer in patients with type 2 diabetes.

Acknowledgements

This study was supported in part by Health Sciences Research Grants for Comprehensive Research on Aging and Health, and Research for Measures for Intractable Diseases from the

Ministry of Health, Labour and Welfare, Leading Project of Biosimulation, and Kobe Translational Research Cluster, and the Knowledge Cluster Initiative from the Ministry of Education, Culture, Sports, Science and Technology, Japan. We thank Use Techno Corporation, Ono Pharmaceutical Co. Ltd., ABBOTT JAPAN Co. Ltd. and Dainippon Pharmaceutical Co. Ltd. for their help in the study.

Conflict of interest

The authors state that they have no conflict of interest.

REFERENCES

[1] The Diabetes Control Complications Trial Research Group, The effect of intensive treatment of diabetes on the development and progression of long-term complications in insulin-dependent diabetes mellitus, New Eng. J. Med. 329 (1993) 977–986.

[2] The Diabetes Control Complications Trial Research Group, Effect of intensive diabetes treatment on nerve conduction in the diabetes control and complications trial, Ann. Neurol. 38 (1995) 869–880.

[3] UK Prospective Diabetes Study (UKPDS) Group, Intensive blood-glucose control with sulphonylureas or insulin compared with conventional treatment and risk of complication in patients with type 2 diabetes (UKPDS33), Lancet 352 (1998) 837–853.

[4] Y. Ohkubo, H. Kishikawa, A. Eiichi, T. Miyata, A. Isami, S. Motoyoshi, et al., Intensive insulin therapy prevents the progression of diabetic microvascular complications in Japanese patients with non-insulin-dependent diabetes mellitus: a randomized prospective 6-year study, Diabetes Res. Clin. Pract. 28 (1995) 103–117.

[5] F.J. Service, R.A. Rizza, J.R. Daube, P.C. O'Brien, P.J. Dyck, Near normoglycaemia improved nerve conduction and vibration sensation in diabetic neuropathy, Diabetologia 28 (1985) 722–727.

[6] A. Pestronk, J. Florence, T. Levine, Al-Lozi, G. Lopate, T. Miller, et al., Sensory exam with a quantitative tuning fork, Neurology 62 (2004) 461–464.

[7] I.S.J. Martina, R. van koningsveld, P.I.M. Schmitz, F.G.A. van der Meche, P.A. van Doorn, For the European inflammatory neuropathy cause and treatment INCAT) group, Measuring vibration threshold with a graduated tuning fork in normal aging and in patients with polyneuropathy, J. Neurol. Neurosurg. Psychiatry 65 (1998) 743–747.

[8] M. Shichiri, H. Kishikawa, Y. Ohkubo, N. Wake, Long-term results of the Kumamoto study on optimal diabetes control in type 2 diabetes patients, Diabetes Care 23 (Suppl. 2) (2000) B21–B29.

[9] Y. Goto, N. Hotta, Y. Shigeta, N. Sakamoto, R. Kikkawa, Effects of aldose reductase inhibitor, epalrestat, on diabetic neuropathy. Clinical benefit and indication for the drug assessed from the results of a placebo-controlled double-blind study, Biomed. Pharmacother. 49 (1995) 269–277.

[10] N. Hotta, K. Sugimura, I. Tsuchida, T. Sano, N. Koh, H. Matsumae, et al., Use of the C64 quantitative tuning fork and the effect of niceritrol in diabetic neuropathy, Clin. Ther. 16 (1994) 1007–1015.

[11] A. Taniguchi, M. Fukushima, M. Sakai, K. Miwa, T. Makita, I. Nagata, et al., Remnant-like particle cholesterol, triglycerides, and insulin resistance in nonobese Japanese type 2 diabetic patients, Diabetes Care 23 (2000) 1766–1769.

[12] M. Fukushima, M. Usami, M. Ikeda, Y. Nakai, A. Taniguchi, T. Matsuura, et al., Insulin secretion and insulin sensitivity at different stages of glucose tolerance: a cross-sectional study of Japanese type 2 diabetes, Metabolism 53 (2004) 831–835.

[13] A.A. Sima, C. Laudadio, Design of controlled clinical trials for diabetic polyneuropathy, Semin. Neurol. 16 (1996) 187–191.

[14] M. James, Kennedy, W. Douglas, Zochodne, Experimental diabetic neuropathy with spontaneous recovery. Is there irreparable damage? Diabetes 54 (2005) 830–837.

[15] S.T. Britland, R.J. Young, A.K. Sharma, B.F. Clarke, Association of painful and painless diabetic polyneuropathy with different patterns of nerve fiber degeneration and regeneration, Diabetes 39 (1990) 898–908.

[16] J.W. Meijer, A.J. Smit, E.V. Sonderen, J.W. Groothoff, W.H. Eisma, T.P. Links, Symptom scoring systems to diagnose distal polyneuropathy in diabetes: the diabetic neuropathy symptom score, Diabet. Med. 19 (2002) 962–965.

[17] S. Yagihashi, Pathology and pathogenic mechanism of diabetic neuropathy, Diabetes Metab. Rev. 11 (1995) 193–225.

[18] S. Thrainsdottir, R.A. Malik, L.B. Dahlin, P. Wiksell, K.F. Eriksson, I. Rosén, J. Petersson, D.A. Greene, G. Sundkvist, Endoneurial capillary abnormalities presage deterioration of glucose tolerance and accompany peripheral neuropathy in man, Diabetes 52 (2003) 2615–2622.

[19] R.A.C. Hughes, T. Umapathi, I.A. Gray, N.A. Gregson, M. Noori, A.S. Pannala, et al., A controlled investigation of the cause of chronic idiopathic axonal polyneuropathy, Brain 127 (2004) 1723–1730.

DIABETES RESEARCH AND CLINICAL PRACTICE 80 (2008) 185–191

available at www.sciencedirect.com

ScienceDirect

journal homepage: www.elsevier.com/locate/diabres

Curcumin inhibits glucose production in isolated mice hepatocytes

Hideya Fujiwara [a], *Masaya Hosokawa* [a,*], *Xiaorong Zhou* [a], *Shimpei Fujimoto* [a], *Kazuhito Fukuda* [a], *Kentaro Toyoda* [a], *Yuichi Nishi* [a], *Yoshihito Fujita* [a], *Kotaro Yamada* [a], *Yuichiro Yamada* [a], *Yutaka Seino* [a,b], *Nobuya Inagaki* [a]

[a] *Department of Diabetes and Clinical Nutrition, Graduate School of Medicine, Kyoto University, 54 Shogoin, Kawahara-cho, Sakyo-ku, Kyoto 606-8507, Japan*
[b] *Kansai Denryoku Hospital, Osaka, Japan*

ARTICLE INFO

Article history:
Received 18 October 2007
Accepted 6 December 2007
Published on line 24 January 2008

Keywords:
Curcumin
Diabetes mellitus
Liver
Mice

ABSTRACT

Curcumin is a compound derived from the spice turmeric, and is a potent anti-oxidant, anti-carcinogenic, and anti-hepatotoxic agent. We have investigated the acute effects of curcumin on hepatic glucose production. Gluconeogenesis and glycogenolysis in isolated hepatocytes, and gluconeogenetic enzyme activity after 120 min exposure to curcumin were measured. Hepatic gluconeogenesis from 1 mM pyruvate was inhibited in a concentration-dependent manner, with a maximal decrease of 45% at the concentration of 25 μM. After 120 min exposure to 25 μM curcumin, hepatic gluconeogenesis from 2 mM dihydroxyacetone phosphate and hepatic glycogenolysis were inhibited by 35% and 20%, respectively. Insulin also inhibited hepatic gluconeogenesis from 1 mM pyruvate and inhibited hepatic glycogenolysis in a concentration-dependent manner. Curcumin (25 μM) showed an additive inhibitory effect with insulin on both hepatic gluconeogenesis and glycogenolysis, indicating that curcumin inhibits hepatic glucose production in an insulin-independent manner. After 120 min exposure to 25 μM curcumin, hepatic glucose-6-phosphatase (G6Pase) activity and phosphoenolpyruvate carboxykinase (PEPCK) activity both were inhibited by 30%, but fructose-1,6-bisphosphatase (FBPase) was not reduced. After 120 min exposure to 25 μM curcumin, phosphorylation of AMP kinase α-Thr^{172} was increased. Thus, the anti-diabetic effects of curcumin are partly due to a reduction in hepatic glucose production caused by activation of AMP kinase and inhibition of G6Pase activity and PEPCK activity.

1. Introduction

Curcumin is the major yellow pigment extracted from turmeric, the powdered rhizome of the herb *curcuma longa*. Turmeric is a spice used extensively in curries and mustards as a coloring and flavoring agent. Curcumin is reported to have a wide range of effects: it is anti-inflammatory [1], anti-oxidant [2,3] anti-hepatotoxic [4], and hypocholesterolemic [5,6]. Curcumin also is reported to have a beneficial effect on blood glucose in diabetic rats [7,8]. However, while elevated hepatic glucose production is

* *Corresponding author.* Tel.: +81 75 751 3560; fax: +81 75 751 4244.
E-mail address: hosokawa@metab.kuhp.kyoto-u.ac.jp (M. Hosokawa).

Abbreviations: DHAP, dihydroxyacetone phosphate; FBP, fructose-1,6-bisphophatase; G6Pase, glucose-6-phosphatase; PEPCK, phosphoenolpyruvate carboxykinase; AMP kinase, adenosine monophosphate activated protein kinase.

0168-8227/$ – see front matter
doi:10.1016/j.diabres.2007.12.004

found frequently in type 2 diabetes, it is not known whether curcumin affects glucose metabolism in the liver. In the present study, we demonstrate that curcumin suppresses hepatic glucose production in an insulin-independent manner in isolated hepatocytes. We also investigated the inhibitory effect of curcumin on the activity of gluconeogenetic enzymes in isolated hepatocytes. Our results show that curcumin activates AMP kinase and suppresses both hepatic glucose-6-phosphatase (G6Pase) and phosphoenolpyruvate carboxykinase (PEPCK), thus inhibiting hepatic glucose output.

2. Materials and methods

2.1. Animals

C57/BL6J mice were purchased from Shimizu (Kyoto, Japan). The mice were allowed access to food, standard rat chow (Oriental Yeast, Osaka, Japan), and water *ad lib*. The mice were housed in an air-controlled (temperature 25 ± 2 °C and 50% humidity) room with a 12 h light/dark-cycle. For gluconeogenesis measurements, the mice were fasted 24 h with free access to water before the experiment. For glycogenolysis measurements, the mice were allowed access to food and water *ad lib* before the experiment.

2.2. Hepatocyte preparation

Liver of 10-week-old mice was perfused through the inferior *vena cava* with a buffer consisting of 140 mM NaCl, 2.6 mM KCl, 0.28 mM Na_2HPO_4, 5 mM glucose, and 10 mM Hepes (pH 7.4) after pentobarbital sodium anesthesia as described previously in Refs. [9,10]. The perfusion was first for 5 min with the buffer supplemented with 0.1 mM EGTA and then for 15 min with the buffer containing 5 mM $CaCl_2$ and 0.2 mg/ml collagenase type 2 (Worthington, Lakewood, NJ). All of the solutions were prewarmed at 37 °C and gassed with a mixture of 95% O_2/5%CO_2, resulting in pH 7.4. The isolated hepatocytes were filtered with nylon mesh (0.75 mm in diameter) and washed twice with the buffer above without collagenase, and suspended in a small volume of DMEM (GIBCO, Rockville, MD) without glucose or pyruvate, and counted. The viability of hepatocytes was evaluated by trypan blue staining. Samples with viability of less than 90% were discarded.

2.3. Hepatic glucose production

For gluconeogenesis measurements, hepatocytes (7.5×10^5) were incubated at 37 °C in a humidified atmosphere (5% CO_2) in 0.5 ml of DMEM without glucose but containing 1 mM pyruvate or 2 mM dihydroxyacetone phosphate (DHAP), 0.24 mM 3-isobutyl-1-methylxanthine in the presence or absence of curcumin or insulin. For glycogenolysis measurements, hepatocytes (7.5×10^5) were incubated at 37 °C in a humidified atmosphere (5% CO_2) in 0.5 ml of DMEM without glucose or pyruvate but containing 0.24 mM 3-isobutyl-1-methylxanthine in the presence or absence of curcumin or insulin. Curcumin was dissolved in DMSO to a concentration in the medium that did not interfere with cell viability (maximally 0.1%, v/v). Incubation was stopped by placing the cells on ice, followed by centrifugation at 4 °C for 60 s at 600 × *g*. The sampling was done at 0, 30, 60, and 120 min. The supernatant was removed, the cells were lysed in 0.1% of SDS in phosphate buffered saline, and the protein content was determined (BCA kit, Pierce). The glucose content of the supernatant was measured by glucose oxidation method (100 Trinder kit, Sigma). The dose–response of curcumin in gluconeogenesis and glycogenolysis were obtained at the incubation time of 120 min.

2.4. DNA synthesis measurement

DNA synthesis of hepatocytes was determined as the uptake of 5-bromo-2′-deoxyuridine (BrdU) according to the instruction manual (Cell Proliferation ELISA, BrdU (colorimetric), Roche Diagnostics, Manheim, Germany). After a 24-h preincubation of isolated hepatocytes with curcumin (25 μM) or vehicle in DMEM without glucose but with 10% fetal calf serum, hepatocytes were incubated for an additional 2 h with BrdU. The hepatocytes were fixed, and BrdU incorporation into DNA in hepatocytes was detected by ELISA. The results of incorporation of BrdU were expressed as photo-absorbance (wavelength 370–492 nm).

2.5. Enzyme activities

Hepatocytes were incubated at 37 °C in a humidified atmosphere (5% CO_2) in DMEM without glucose but containing 1 mM pyruvate and 0.24 mM 3-isobutyl-1-methylxanthine in the presence of 25 μM curcumin or vehicle (DMSO) for 120 min. Incubation was stopped by placing the cells on ice followed by centrifugation at 4 °C for 60 s at 600 × *g*. The supernatant was removed, and the cells were homogenized using a glass/Teflon homogenizer. In the microsomal preparation for the G6Pase assay, 50 mM Tris–HCl, pH 7.5, containing 250 mM sucrose, and 0.2 mM EDTA, was used as the homogenizing buffer [11]. For assay of G6Pase, liver microsomal fraction was prepared as follows: homogenate obtained as above was centrifuged at 20,000 × *g* for 20 min at 4 °C, and was then ultracentrifuged at 105,000 × *g* for 1 h at 4 °C. The resulting sediments were used for G6Pase assay [11]. The G6Pase activity was measured with intact microsomal preparation. Activity of G6Pase was determined as described by Passonneau and Lowry [12].

For liver PEPCK and fructose-1,6-bisphophatase (FBPase) assays, the homogenizing buffer contained 0.1 M Tris–HCl, pH 7.5, 0.15 M KCl, 5 mM EDTA, 5 mM dithiothreitol, and 5 mM $MgSO_4$ [11]. The homogenate was centrifuged at 105,000 × *g* for 1 h at 4 °C, and the supernatant was collected. Activity of FBPase was determined as described by Passonneau and Lowry [12].

Activity of PEPCK was determined as described by Nakagawa and Nagai [13]. All enzyme activity was measured photometrically using BIO-RAD Benchmark Plus.

Enzyme activities are expressed as the number of substrate molecules converted by 1 mg cytosolic or microsomal protein per minute. The liver microsomal fraction was solubilized by addition of 0.1% SDS before protein determination.

2.6. Immunoblotting analysis

Hepatocytes were incubated at 37 °C in a humidified atmosphere (5% CO_2) in 10 ml of DMEM without glucose but

containing 1 mM pyruvate and 0.24 mM 3-isobutyl-1-methylxanthine in the presence of 25 μM curcumin or vehicle (DMSO) for 120 min. Incubation was stopped by placing the cells on ice followed by centrifugation at 4 °C for 60 s at 600 × g. The supernatant was removed, and the cells were homogenized in ice-cold lysis buffer (50 mM Tris–HCl, pH 7.4, 50 mM NaF, 1 mM sodium pyrophosphate, 1 mM EDTA, 1 mM EGTA, 1 mM dithiothreitol, 0.1 mM benzamidine, 0.1 mM phenylmethylsulfonylfluoride, 0.2 mM sodium vanadate, 250 mM mannitol, 1% Triton X-100, and 5 μg/ml soybean trypsin inhibitor). The cell lysates were sonicated twice for 10 s and centrifuged at 13,000 × g for 5 min. The pellets were discarded, and supernatants were assayed for protein concentration. Equal amounts of proteins (50 μg) were subjected to SDS-polyacrylamide (8%) gel electrophoresis and transferred onto nitrocellulose membranes (PROTRAN, Schleicher & Schuell) by electroblotting. After pre-incubation with blocking buffer (PBS containing 0.1% Tween 20 and 5% nonfat dry milk) for 2 h at room temperature, blotted membranes were incubated with each primary antibody (phospho-AMP kinase α-Thr^{172} antibody or AMP kinase α antibody, Cell Signaling Technology, Danvers, MA) overnight at 4 °C, followed by washing twice with blocking buffer. Membranes were then incubated with a horseradish peroxidase-linked anti-rabbit IgG (Amersham) for 1 h at room temperature, washed twice in PBS containing 0.04% Tween 20, and visualized by ECL Western blotting detection reagents (Amersham). Densitometry was carried out to measure band intensities and phosphorylated AMP kinase α-Thr^{172} was normalized by the levels of AMP kinase α protein.

2.7. *Materials*

Curcumin was purchased from Wako Chemicals (Osaka, Japan). Standard rat chow was from Oriental Yeast (Osaka, Japan). Human insulin was from Novo-Nordisk (Copenhagen, Denmark). All other chemicals were of reagent grade.

2.8. *Statistical analysis*

Results are mean ± S.E.M. (n = number of animals). Statistical significance was evaluated using two-tailed Student's t-tests. Differences among groups were also statistically examined by one-way ANOVA (Fisher's PLSD test). $P < 0.05$ was considered significant.

2.9. *Ethical considerations*

All studies were performed in the laboratories of the Department of Diabetes and Clinical Nutrition, Kyoto University, in accordance with the Declaration of Helsinki.

3. Results

3.1. *Effect of curcumin on hepatic gluconeogenesis in freshly isolated hepatocytes*

Fig. 1A shows the time course of inhibition by curcumin of hepatic gluconeogenesis from pyruvate. After 30, 60, and 120 min exposure to 25 μM curcumin, hepatic gluconeogenesis was significantly inhibited by approximately 45%, 40%, and 45%, respectively. The viability of the hepatocytes was not affected by 120 min exposure to 25 μM curcumin (control: 78 ± 1% vs. curcumin: 79 ± 2%). Fig. 1B shows the time course of inhibition by curcumin of hepatic gluconeogenesis from dihydroxyacetone phosphate. After 120 min exposure to 25 μM curcumin, hepatic gluconeogenesis was significantly inhibited by approximately 35%.

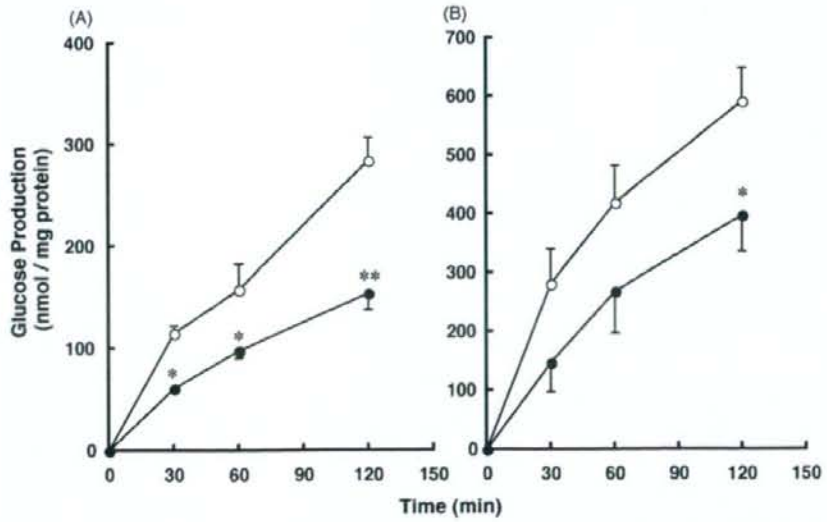

Fig. 1 – Time course of inhibition in hepatic gluconeogenesis from 1 mM pyruvate (A) and 2 mM DHAP (B). Isolated hepatocytes from fasted mice were incubated in the presence of 25 μM curcumin or vehicle for 2 h. Glucose content in supernatant was measured by glucose oxidation method. Each point shows mean ± S.E.M. (n = 6). *$P < 0.05$, **$P < 0.01$ compared with control by unpaired Student's t-test. Control (○), curcumin (●).

As shown in Fig. 2, curcumin inhibited hepatic gluconeogenesis from pyruvate at the incubation time of 120 min in a concentration-dependent manner.

As shown in Fig. 3, after 120 min exposure to insulin, hepatic gluconeogenesis from pyruvate was inhibited in a concentration-dependent manner. After 120 min exposure to various concentrations of insulin (0.1, 1, and 10 nM) in the presence of 25 μM curcumin, hepatic gluconeogenesis from pyruvate was further inhibited by approximately 45% when compared to that in the absence of 25 μM curcumin.

3.2. *Effect of curcumin on DNA synthesis in isolated hepatocytes*

To determine whether curcumin is toxic to hepatocytes, we examined the effect of curcumin on DNA synthesis in isolated hepatocytes. After 24 h exposure to 25 μM curcumin, BrdU incorporation into DNA in isolated hepatocytes was not decreased compared to control, indicating no suppressive effects of curcumin on DNA synthesis (Fig. 4).

3.3. *Effect of curcumin on hepatic glycogenolysis in freshly isolated hepatocytes*

Fig. 5A shows the time course of inhibition by curcumin of hepatic glucose production from glycogenolysis. After 60 and 120 min exposure to 25 μM curcumin, hepatic glycogenolysis was significantly inhibited by approximately 10% and 20%, respectively. As shown in Fig. 5B, curcumin inhibited hepatic glycogenolysis at the incubation time of 120 min in a concentration-dependent manner. As shown in Fig. 6, after

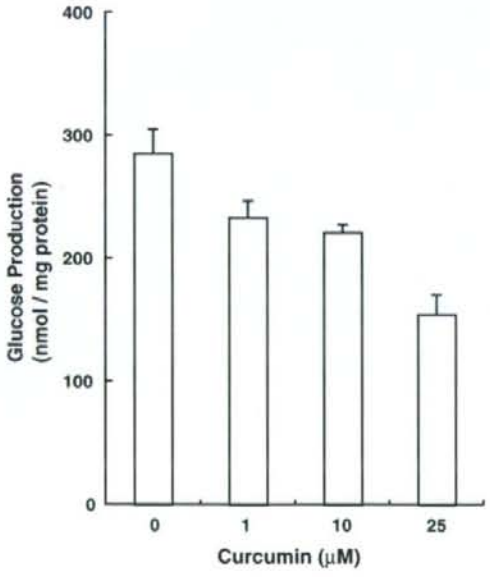

Fig. 2 – Concentration-dependence of inhibition in gluconeogenesis from 1 mM pyruvate by curcumin at the incubation time of 120 min in isolated mice hepatocytes. Each point shows mean ± S.E.M. ($n = 6$). $P < 0.001$ by one-way ANOVA.

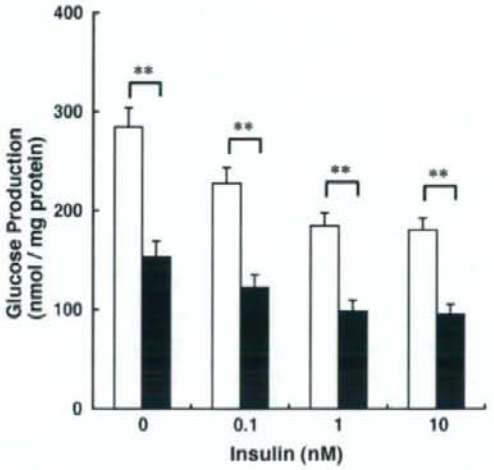

Fig. 3 – Concentration-dependence of inhibition in gluconeogenesis from 1 mM pyruvate by insulin in the presence and absence of 25 μM curcumin in isolated mice hepatocytes. Each point shows mean ± S.E.M. ($n = 6$). $P < 0.001$ by one-way ANOVA. **$P < 0.01$ compared with insulin alone by unpaired Student's t-test. Insulin alone (open bar), insulin plus curcumin (closed bar).

120 min exposure to insulin, hepatic glycogenolysis was inhibited in a concentration-dependent manner. After 120 min exposure to various concentrations of insulin (0.1, 1, and 10 nM) in the presence of 25 μM curcumin, hepatic glycogenolysis was further inhibited by approximately 20% compared to that in the absence of 25 μM curcumin.

3.4. *Effect of curcumin on activities of hepatic gluconeogenetic enzymes*

To further investigate inhibition of hepatic glucose production by curcumin, we measured the activities of key gluconeogenetic enzymes, G6Pase, FBPase, and PEPCK. After 120 min exposure to 25 μM curcumin, hepatic G6Pase activity and PEPCK activity were significantly inhibited by approximately 30%, but FBPase was not inhibited (Fig. 7).

3.5. *Effect of curcumin on phosphorylation of AMP kinase*

AMP kinase activation was monitored in Western blots by staining with a specific antibody against phosphorylated Thr^{172} of AMP kinase α, which is essential for AMP kinase activity. After 120 min exposure to 25 μM curcumin, phosphorylation of AMP kinase α-Thr^{172} was significantly increased by 70% when normalized by total content of AMP kinase α, clearly indicating curcumin activation of AMP kinase (Fig. 8).

4. Discussion

This is the first study to show that curcumin reduces hepatic glucose production. Our results demonstrate that curcumin

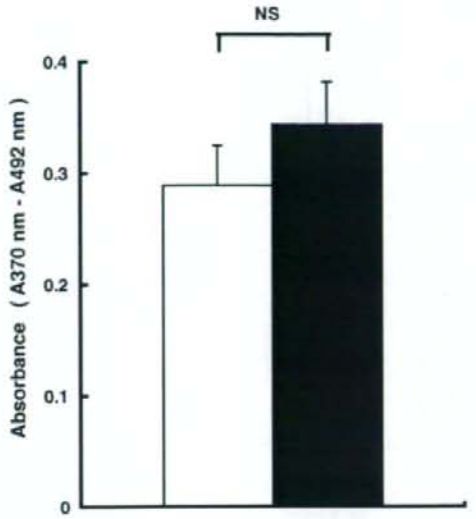

Fig. 4 – The effect of curcumin on DNA synthesis in isolated hepatocytes. After 24-h pre-incubation of isolated mice hepatocytes with 25 μM curcumin or vehicle in DMEM without glucose but with 10% fetal calf serum, hepatocytes were incubated for an additional 2 h with BrdU. The results of incorporation of BrdU were expressed as photo-absorbance (wavelength 370–492 nm). Control (open bar), curcumin (closed bar).

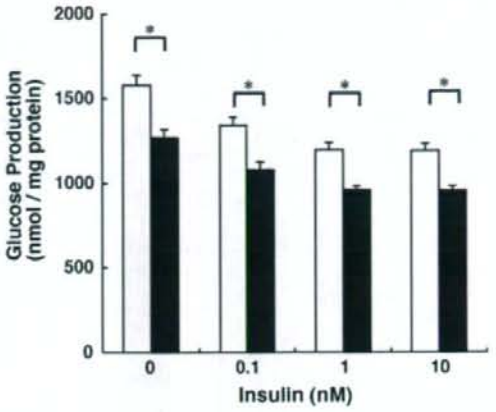

Fig. 6 – Concentration-dependence of inhibition in glycogenolysis by insulin in the presence and absence of 25 μM curcumin at the incubation time of 120 min in isolated mice hepatocytes. Each point shows mean ± S.E.M. ($n = 6$). $P < 0.001$ by one-way ANOVA. *$P < 0.05$ compared with insulin alone by unpaired Student's t-test. Insulin alone (open bar), insulin plus curcumin (closed bar).

inhibits both hepatic gluconeogenesis and glycogenolysis by suppressing both G6Pase activity and PEPCK activity. As curcumin had no suppressive effect on DNA synthesis in isolated hepatocytes, the inhibition of hepatic glucose production should not be a toxic effect. Indeed, Shen et al.

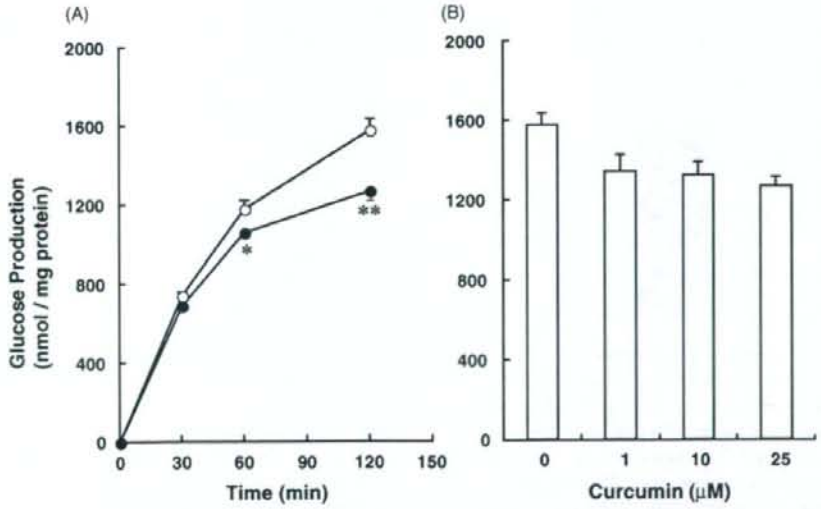

Fig. 5 – (A) Time course of inhibition of hepatic glucose production from glycogenolysis by curcumin. Isolated hepatocytes from fed mice were incubated in the presence of 25 μM curcumin or vehicle for 2 h. Glucose content in supernatant was measured by glucose oxidation method. Each point shows mean ± S.E.M. ($n = 5$). *$P < 0.05$, **$P < 0.01$ compared with control by unpaired Student's t-test. Control (○), curcumin (●). (B) Concentration-dependence of inhibition of glycogenolysis by curcumin at the incubation time of 120 min in isolated mice hepatocytes. Each point shows mean ± S.E.M. ($n = 6$). $P < 0.05$ by one-way ANOVA.

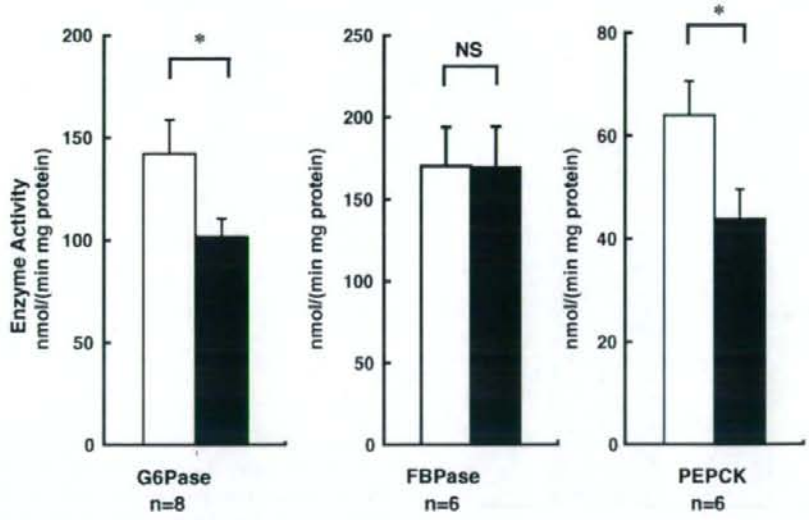

Fig. 7 – Effects of curcumin on hepatic gluconeogenetic activities of G6Pase, FBPase, and PEPCK in isolated mice hepatocyte. Isolated hepatocytes from fasted mice were incubated in the presence of 25 μM curcumin or vehicle for 2 h. All enzyme activities were measured photometrically. Enzyme activities are expressed as the number of substrate molecules converted by 1 mg cytosolic or microsomal protein per minute. Each point shows mean ± S.E.M. *P < 0.05 compared with control by unpaired Student's t-test. Control (open bar), curcumin (closed bar).

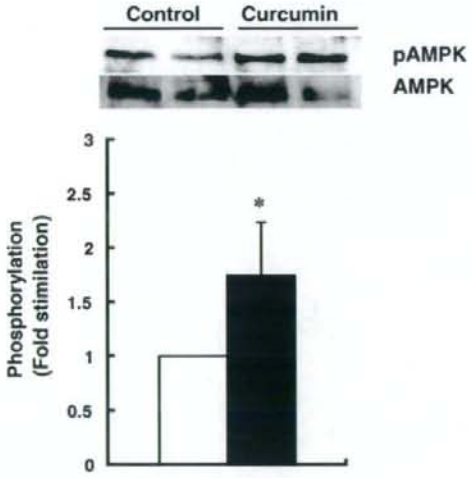

Fig. 8 – Effect of curcumin on activation of AMP kinase in isolated mice hepatocytes. AMP kinase activation was monitored in Western blots by staining with a specific antibody against phosphorylated Thr^{172} of AMP kinase α. After 120 min exposure to 25 μM curcumin, the level of phosphorylation of AMP kinase α-Thr^{172} (pAMPK) was significantly increased by 70% when normalized by total content of AMP kinase α (AMPK), and is expressed as fold stimulation over the control (mean ± S.E.M., n = 5) (lower panel). Upper panel shows a representative immunoblot of pAMPK and AMPK in hepatocytes from two mice in each group. *P < 0.05 compared with control by unpaired Student's t-test. Control (open bar), curcumin (closed bar).

recently reported a protective effect of curcumin against warm ischemia/reperfusion injury in rat liver [14].

Arun and Nalini reported that curcumin reduced blood glucose in alloxan-induced diabetic rats [7], but the mechanism of the anti-diabetic action was left unclear in that study. In the present study, insulin was found to dose-dependently inhibit hepatic gluconeogenesis, reaching a plateau at a concentration of 10 nM. In the presence of 10 nM insulin, the addition of 25 μM curcumin enchanced the inhibitory effect of insulin on hepatic gluconeogenesis, demonstrating that curcumin inhibits hepatic gluconeogenesis by a pathway independent of insulin signaling. Thus, curcumin is an insulin-sentitizing agent.

Recently, the major effect of metformin, a biguanide, was reported to be inhibition of hepatic G6Pase activity and hepatic glucose production in rats fed a high-fat diet [15]. Zhou et al. reported that metformin activated AMP kinase in hepatocytes [16]. The activation of AMP kinase is known to suppress gene expression of G6Pase and PEPCK and to inhibit hepatic glucose production in an insulin-independent manner [17,18]. In the present study, curcumin was found to inhibit both G6Pase and PEPCK activity; we therefore measured the effect of curcumin on AMP kinase activity to clarify the underlying mechanism. Zang et al. reported that resveratrol, a polyphenol and an anti-oxidant, which is a key component in red wine, stimulates AMP kinase in hepatoma HepG2 cells [19]. Kim et al. reported that cryptotanshinone, another anti-oxidant and a diterpene, which was originally isolated from dried roots of *Salvia mlitorrhiza* Bunge, showed anti-diabetic effects through activation of AMP kinase [20]. Considering these findings together, the potent anti-oxidant effect of curcumin may

well be involved in the activation of AMP kinase. Further investigation is required to clarify the anti-diabetic action of curcumin in hepatocytes.

Biguanide sometimes shows the lethal adverse effect of lactic acidosis in diabetic patients when prescribed inappropriately. On the other hand, since curcumin is derived from an extensively used dietary spice, the compound may well be safely administered to humans. Indeed, Sharma et al. administered oral daily curcumin to advanced colorectal cancer patients without major adverse effects [21]. Cheng et al. also administered oral daily curcumin to patients with high risk or pre-malignant lesions [22].

Considered together with our results, these data suggest that curcumin might provide a valuable new therapy in the treatment of type 2 diabetes.

Acknowledgements

This study was supported in part by Grants-in-Aids for Scientific Research from the Ministry of Education, Culture, Sports, Science and Technology of Japan; Health and Labour Sciences Research Grants for Research on Human Genome, Tissue Engineering, and Food Biotechnology from the Ministry of Health, Labor and Welfare of Japan; and Health and Labour Sciences Research Grants for Comprehensive Research on Aging and Health from the Ministry of Health, Labor and Welfare of Japan.

Conflict of interest

The authors state that they have no conflict of interest.

REFERENCES

[1] R.C. Srimal, B.N. Dhawan, Pharmacology of diferuloyl methane (curcumin), a non-steroidal anti-inflammatory agent, J. Pharm. Pharmacol. 25 (1973) 447–452.

[2] B. Joe, B.R. Lokesh, Role of capsaicin, curcumin and dietary n-3 fatty acids in lowering the generation of reactive oxygen species in rat peritoneal macrophages, Biochim. Biophys. Acta 1224 (1994) 255–263.

[3] A.C. Reddy, B.R. Lokesh, Studies on the inhibitory effects of curcumin and eugenol on the formation of reactive oxygen species and the oxidation of ferrous iron, Mol. Cell. Biochem. 137 (1994) 1–8.

[4] Y. Kiso, Y. Suzuki, N. Watanabe, Y. Oshima, H. Hikino, Antihepatotoxic principles of *Curcuma longa* rhizomes, Planta Med. 49 (1983) 185–187.

[5] D.S. Rao, N.C. Sekhara, M.N. Satyanarayana, M. Srinivasan, Effect of curcumin on serum and liver cholesterol levels in the rat, J. Nutr. 100 (1970) 1307–1315.

[6] T.N. Patil, M. Srinivasan, Hypocholesteremic effect of curcumin in induced hypercholesteremic rats, Indian J. Exp. Biol. 9 (1971) 167–169.

[7] N. Arun, N. Nalini, Efficacy of turmeric on blood sugar and polyol pathway in diabetic albino rats, Plant Foods Hum. Nutr. 57 (2002) 41–52.

[8] T. Nishiyama, T. Mae, H. Kishida, M. Tsukagawa, Y. Mimaki, M. Kuroda, et al., Curcuminoids and sesquiterpenoids in turmeric (*Curcuma longa* L.) suppress an increase in blood glucose level in type 2 diabetic KK-Ay mice, J. Agric. Food Chem. 53 (2005) 959–963.

[9] M. Hosokawa, B. Thorens, Glucose release from GLUT2-null hepatocytes: characterization of a major and a minor pathway, Am. J. Physiol. Endocrinol. Metab. 282 (2002) E794–E801.

[10] M. Uldry, M. Ibberson, M. Hosokawa, B. Thorens, GLUT2 is a high affinity glucosamine transporter, FEBS Lett. 524 (2002) 199–203.

[11] K. Aoki, T. Saito, S. Satoh, K. Mukasa, M. Kaneshiro, S. Kawasaki, et al., Dehydroepiandrosterone suppresses the elevated hepatic glucose-6-phosphatase and fructose-1,6-bisphosphatase activities in C57BL/Ksj-db/db mice: comparison with troglitazone, Diabetes 48 (1999) 1579–1585.

[12] J.V. Passoneau, O.H. Lowry, Enzymic Analysis: A Practical Guide by Passoneau JV and Lowry OH., Humana Press, Totowa, NJ, 1993, pp. 249–253.

[13] H. Nakagawa, K. Nagai, Cold adaptation. I. Effect of cold-exposure on gluconeogenesis, J. Biochem. (Tokyo) 69 (1971) 923–934.

[14] S.Q. Shen, Y. Zhang, J.J. Xiang, C.L. Xiong, Protective effect of curcumin against liver warm ischemia/reperfusion injury in rat model is associated with regulation of heat shock protein and antioxidant enzymes, World J. Gastroenterol. 13 (2007) 1953–1961.

[15] G. Mithieux, L. Guignot, J.C. Bordet, N. Wiernsperger, Intrahepatic mechanisms underlying the effect of metformin in decreasing basal glucose production in rats fed a high-fat diet, Diabetes 51 (2002) 139–143.

[16] G. Zhou, R. Myers, Y. Li, Y. Chen, X. Shen, J. Fenyk-Melody, et al., Role of AMP-activated protein kinase in mechanism of metformin action, J. Clin. Invest. 108 (2001) 1167–1174.

[17] P.A. Lochhead, I.P. Salt, K.S. Walker, D.G. Hardie, C. Sutherland, 5-Aminoimidazole-4-carboxamide riboside mimics the effects of insulin on the expression of the 2 key gluconeogenic genes PEPCK and glucose-6-phosphatase, Diabetes 49 (2000) 896–903.

[18] T. Yamauchi, J. Kamon, Y. Minokoshi, Y. Ito, H. Waki, S. Uchida, et al., Adiponectin stimulates glucose utilization and fatty-acid oxidation by activating AMP-activated protein kinase, Nat. Med. 8 (2002) 1288–1295.

[19] M. Zang, S. Xu, K.A. Maitland-Toolan, A. Zuccollo, X. Hou, B. Jiang, et al., Polyphenols stimulate AMP-activated protein kinase, lower lipids, and inhibit accelerated atherosclerosis in diabetic LDL receptor-deficient mice, Diabetes 55 (2006) 2180–2191.

[20] E.J. Kim, S.N. Jung, K.H. Son, S.R. Kim, T.Y. Ha, M.G. Park, et al., Antidiabetes and antiobesity effect of cryptotanshinone via activation of AMP-activated protein kinase, Mol. Pharmacol. 72 (2007) 62–72.

[21] R.A. Sharma, S.A. Euden, S.L. Platton, D.N. Cooke, A. Shafayat, H.R. Hewitt, et al., Phase I clinical trial of oral curcumin: biomarkers of systemic activity and compliance, Clin. Cancer Res. 10 (2004) 6847–6854.

[22] A.L. Cheng, C.H. Hsu, J.K. Lin, M.M. Hsu, Y.F. Ho, T.S. Shen, et al., Phase I clinical trial of curcumin, a chemopreventive agent, in patients with high-risk or pre-malignant lesions, Anticancer Res. 21 (2001) 2895–2900.

Available online at www.sciencedirect.com
ScienceDirect
Biochemical and Biophysical Research Communications 367 (2008) 793–798
BBRC
www.elsevier.com/locate/ybbrc

GLP-1 receptor signaling protects pancreatic beta cells in intraportal islet transplant by inhibiting apoptosis

Kentaro Toyoda [a], Teru Okitsu [b], Shunsuke Yamane [a], Taeko Uonaga [a], Xibao Liu [a], Norio Harada [a], Shinji Uemoto [c], Yutaka Seino [d], Nobuya Inagaki [a,e,*]

[a] *Department of Diabetes and Clinical Nutrition, Graduate School of Medicine, Kyoto University, 54 Kawahara-cho, Shogoin Sakyo-ku, Kyoto 606-8507, Japan*
[b] *Transplantation Unit, Kyoto University Hospital, Kyoto 606-8507, Japan*
[c] *Department of Surgery, Graduate School of Medicine, Kyoto University, Kyoto 606-8507, Japan*
[d] *Kansai Denryoku Hospital, Osaka 553-0003, Japan*
[e] *CREST of Japan Science and Technology Cooperation (JST), Kyoto, Japan*

Received 6 January 2008
Available online 22 January 2008

Abstract

To clarify the cytoprotective effect of glucagon-like peptide-1 receptor (GLP-1R) signaling in conditions of glucose toxicity *in vivo*, we performed murine isogenic islet transplantation with and without exendin-4 treatment. When a suboptimal number of islets (150) were transplanted into streptozotocin-induced diabetic mice, exendin-4 treatment contributed to the restoration of normoglycemia. When 50 islets expressing enhanced green fluorescent protein (EGFP) were transplanted, exendin-4 treatment reversed loss of both the number and mass of islet grafts one and 3 days after transplantation. TUNEL staining revealed that exendin-4 treatment reduced the number of apoptotic beta cells during the early posttransplant phase, indicating that GLP-1R signaling exerts its cytoprotective effect on pancreatic beta cells by inhibiting their apoptosis. This beneficial effect might be used both to ameliorate type 2 diabetes and to improve engraftment rates in clinical islet transplantation.

Keywords: Exendin-4; Glucagon-like peptide-1; Cytoprotection; Apoptosis; Enhanced green fluorescent protein; Islet transplantation; Islet engraftment

Glucagon-like peptide-1 (GLP-1) is a physiological incretin, an intestinal hormone released in response to nutrient ingestion that stimulates glucose-dependent insulin secretion [1,2]. Recent studies have demonstrated that GLP-1 has beneficial effects on pancreatic beta cells [3–6], one of which is inhibition of apoptosis of native beta cells. *In vitro* studies have shown that GLP-1 receptor (GLP-1R) signaling has various beneficial actions such as ameliorating ER stress [7,8] and oxidative stress [9]. However, demonstration of the *in vivo* cytoprotective effect in an animal model of type 2 diabetes (T2DM) is problematic because enhancement of GLP-1R signaling reduces blood glucose levels due to its insulinotropic action [4,5], glucagonostatic action on alpha cells [10], and improvement of insulin sensitivity [11], which makes it difficult to evaluate the cytoprotective effects in the same conditions of glucose toxicity.

To clarify the cytoprotective effect of GLP-1R signaling *in vivo*, we used a murine isogenic islet transplantation model using a suboptimal number of islets together with exendin-4 treatment, a degradation-resistant GLP-1 analog [12]. As isogenic islet grafts in the natural course of the early posttransplant period are easily lost due to various physiological stress [13], various suboptimal number of islet transplantation can lead proper engraftment during the transplantation process without regard for the effects of improved blood glucose levels following transplantation

* Corresponding author. Address: Department of Diabetes and Clinical Nutrition, Graduate School of Medicine, Kyoto University, 54 Kawahara-cho, Shogoin Sakyo-ku, Kyoto 606-8507, Japan. Fax: +81 75 751 4244.
E-mail address: inagaki@metab.kuhp.kyoto-u.ac.jp (N. Inagaki).

0006-291X/$ - see front matter © 2008 Elsevier Inc. All rights reserved.
doi:10.1016/j.bbrc.2008.01.046

of an optimal number of islets. When a higher suboptimal mass of islets is transplanted, blood glucose levels remain high during the early posttransplant period, changing to normoglycemic only during the late posttransplantation period if the engrafted mass is sufficient but remaining in the hyperglycemic state if the engrafted mass is insufficient. Thus, when a suboptimal number of islets are transplanted together with exendin-4 treatment in the early posttransplant period when the recipient is hyperglycemic, its indirect action on glucose tolerance can be excluded and its cytoprotective effect can be evaluated by monitoring the blood glucose levels. In addition, bio-imaging technology permits comparison of the number and mass of islets before and after transplantation.

In the present study, we evaluated the cytoprotective effect of GLP-1R signaling *in vivo* in pancreatic beta cells using a murine isogenic islet transplantation model. We used a suboptimal mass of transplanted islets with and without exendin-4 treatment, and monitored blood glucose levels. We also compared the number and mass of islet grafts with and without exendin-4 treatment under conditions of hyperglycemia.

Materials and methods

Animal care. All experiments were approved by the Kyoto University Animal Care Committee.

Animals. Male C57BL/6JJcl mice (CREA, Japan) aged 8–10 weeks were used as recipients and donors. Male transgenic C57BL/6-EGFP mice aged 8–10 weeks were also used as donors. The mice were obtained from Dr. Masaru Okabe (Research Institute for Microbial Diseases, Osaka University, Osaka, Japan) [14]. Recipient animals were rendered diabetic by a single intraperitoneal injection of streptozotocin (Sigma–Aldrich, USA), 120 mg/kg body weight, freshly dissolved in 10 mM citrate buffer (pH 4.2). Mice with a blood glucose concentration greater than 20 mmol/l for 2 consecutive days were used as recipients. Blood glucose concentrations were determined by glucose meter (Glucocard, Arkley, Japan).

Islet isolation, islet transplantation, and exendin-4 treatment. Islets were isolated, as previously described [15]. Recipient mice were anesthetized by isoflurane (Forane, Abott, Japan). Fresh islets in a volume of 400 μl PBS solution were injected into the portal vein and transplanted into the right hepatic lobe as previously described [15,16]. Exendin-4 at a dosage of 1.0 nmol/kg body weight was administered intraperitoneally once daily in the morning for 14 days.

Oral glucose tolerance test (OGTT). After fasting for 16 h, a basal blood sample was collected and the mice received glucose (1.5 g/kg body weight) orally; additional blood samples were collected at 15, 30, 60, 90, and 120 min after glucose loading.

Evaluation of number and mass of EGFP-expressing islet grafts. Islets isolated from transgenic C57BL/6-EGFP mice were first observed by fluorescence microscope BZ-8000 (KeyEnce, Japan) before transplantation; the area of fluorescence was measured using Image J software (National Institute of Mental Health, USA). Livers bearing islet grafts were removed and sectioned into 500-μm slices and serialized; digitalized photographs of all sections were taken. The number of EGFP-positive islets in each liver section was then counted, excepting those appearing by their position to be part of an islet in an adjacent section. The total area of fluorescence of all islets was then measured.

Measurement of beta-cell mass using immunohistochemistry. The right hepatic lobes were fixed, embedded in paraffin, cut in blocks at regular intervals, and sectioned into 5-μm sections. Deparaffinized sections were incubated with a polyclonal guinea pig anti-insulin antibody (Dako, USA), then with a biotinylated goat anti-guinea pig antibody (Vector, USA), and then with a streptavidin peroxidase conjugate and substrate kit (Dako). The total liver area and total insulin-positive beta-cell area were quantified using Image J software.

Apoptosis detection. TUNEL staining was performed using Apoptosis detection Kit (Takara Bio, Japan).

Statistical analyses. All data are presented as means ± SEM. Statistical analyses were performed by an unpaired *t*-test. *p* value of less than 0.05 was considered significant.

Results

Exendin-4 decreased the number of islet grafts required to restore normoglycemia

To evaluate the cytoprotective effect of GLP-1R signaling during the early posttransplant phase, we performed isogenic islet transplantation and observed blood glucose levels during the late posttransplant phase. Previous reports have shown that transplantation of only 75 islets can normalize blood glucose levels if the majority becomes engrafted [17], but because many islets are lost due to various stress such as glucotoxicity, transplantation of 75 islets is insufficient for restoration of normoglycemia. In our preliminary experiments, while some recipients showed improved blood glucose levels when 200 islets were transplanted (data not shown), no recipients showed any change in blood glucose levels when 150 islets were transplanted (Fig. 1A). Thus, 150 islets was chosen as an appropriate suboptimal number for use in these transplantation experiments. In addition, all mice transplanted with 150 islets together with exendin-4 treatment became hyperglycemic soon after transplantation but became normoglycemic approximately 14 days after transplantation (Fig. 1A). The responsibility of the islet grafts in exendin-4-treated mice in maintenance of glucose tolerance is demonstrated by the immediate return to hyperglycemia after removal the right hepatic lobe (Fig. 1B). In addition, OGTT was similar in mice receiving 150 islets with exendin-4 treatment and sham-operated control mice (Fig. 1C). These results indicate that exendin-4 treatment played a crucial role in the restoration of normoglycemia by protecting the transplanted islets from damage during the early posttransplant phase.

Detection of fluorescence of transplanted Islets of transgenic C57BL/6-EGFP mice

To clarify the cytoprotective effect of exendin-4 *in vivo*, we established a novel system whereby the total number and the total mass of islets can be compared before and after transplantation by using fluorescent islets isolated from transgenic C57BL/6-EGFP mice. These mice exhibited normal pancreas and islet morphology and well as normal glucose tolerance by OGTT (data not shown).

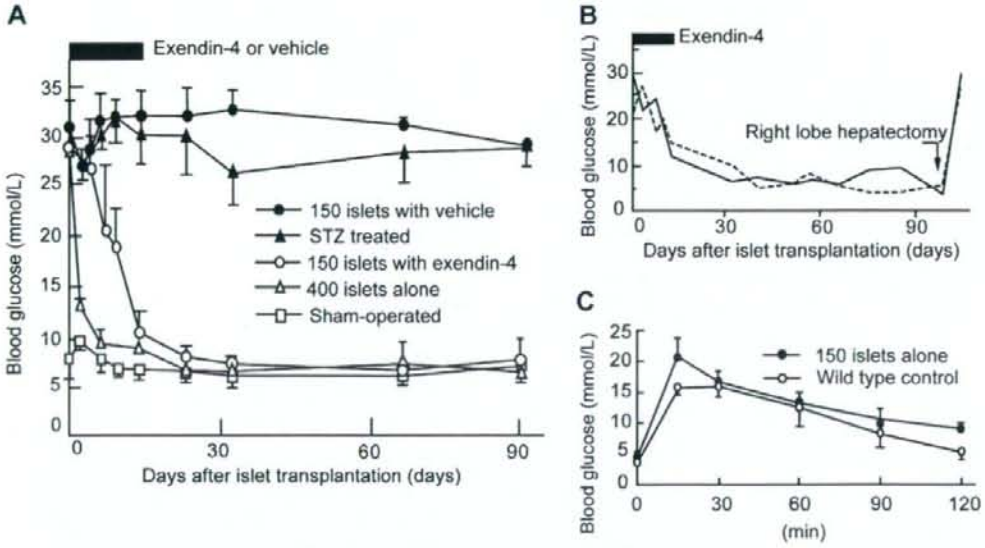

Fig. 1. Exendin-4 reduced the number of islets required for transplantation to restore normoglycemia in STZ-induced diabetic mice. (A) Blood glucose concentrations were measured in mice transplanted with 150 islets together with 1 nmol/kg exendin-4 treatment (open circles, $n = 4$), 400 islets alone (filled triangles, $n = 5$), 150 islets alone (filled circles, $n = 3$), STZ-treated only (filled triangles, $n = 5$), and Sham-operated C57BL/6 mice (open squares, $n = 5$). (B) Right hepatic lobe was resected from two recipients transplanted with 150 islets together with exendin-4 treatment on Day 90 to clarify the effect of the islet grafts on glycemic control. (C) OGTT was performed on Day 30 in recipients transplanted with 150 islets together with exendin-4 treatment and in sham-operated wild-type C57BL/6 mice ($n = 3$ for each).

Transplanted islets of transgenic C57BL/6-EGFP mice are traceable and measurable in both number and mass

To confirm traceability and measurability of the transplanted islets, intraportal transplantation of islets isolated from transgenic C57BL/6-EGFP mice was performed. One day and three days after transplantation, the right hepatic lobe was resected and sliced, and each slice was photographed by fluorescence microscope (Fig. 2A–C). Liver slices containing islet grafts were then immunostained for insulin. The area of fluorescence (Fig. 2A) coincided with that of the islet beta cells stained for insulin (Fig. 2B), demonstrating traceability of the islets. The number of islet grafts in the liver after transplantation was then compared. When 25, 50, or 75 islets were transplanted, the total number of islet grafts detected in the liver was 24.3 ± 0.3, 48.7 ± 0.8 and 73.3 ± 0.3, respectively ($n = 3$ for each), demonstrating a significant ($p < 0.0001$), strong correlation ($r = 1.000$) between the number of detected islet grafts in the liver and the number of transplanted islets (Fig. 2E). In addition, because the area of fluorescence coincided with that of immunostained islets (Fig. 2A–C), the total area of fluorescence reflected the total area mass of the islets, allowing comparison of total islet mass before and after transplantation. When 25, 50, and 75 islets were transplanted, the total area mass of islets before transplantation was 2.01 ± 0.04, 4.11 ± 0.01, and 5.89 ± 0.09 (mm^2), respectively, while that of islet grafts in the liver were 2.00 ± 0.02, 4.28 ± 0.07, and 6.08 ± 0.03 (mm^2), respectively ($n = 3$ for each), demonstrating a significant ($p < 0.0001$), strong ($r = 0.998$) correlation between before and after transplantation (Fig. 2F).

Exendin-4 reduced loss of transplanted islets from transgenic C57BL/6-EGFP mice during the early posttransplant phase

To exclude the indirect effect of exendin-4 through its effect on blood glucose levels, we reduced the number of the transplanted islets to 50. When 50 islets of transgenic C57BL/6-EGFP mice were transplanted with or without treatment of exendin-4 into STZ-induced diabetic mice, the blood glucose levels were not significantly different on 1 day (Day 1) ($n = 3$, 27.1 ± 0.3 vs 27.8 ± 0.1 (mmol/l), $p = 0.193$) or 3 days (Day 3) after transplantation ($n = 3$, 28.7 ± 0.2 vs 28.7 ± 0.3 (mmol/l), $p = 0.936$). The number and the total area mass of the islet grafts in livers resected on Day 1 (figure not shown) and Day 3 (Fig. 3A and B) were then examined. The number of islet grafts with treatment of exendin-4 (Ex(+)) showed 9.4% and 19.9% increases on Day 1 ($n = 3$ for each, 46.7 ± 0.51 vs 42.0 ± 0.33, $p < 0.05$) and Day 3 ($n = 3$ for each, 44.6 ± 0.36 vs 34.7 ± 0.84, $p < 0.01$) (Fig. 3C) compared to those without treatment (Ex(−)). Ex(+) islet grafts exhibited 29.0% and 31.9% more total area mass on Day 1 ($n = 3$ for each, $69.5 \pm 2.5\%$ vs $53.3 \pm 2.1\%$ (normalized to the total fluorescence area mass before transplantation), $p < 0.05$) and Day 3 ($n = 3$ for each, $64.5 \pm 2.6\%$ vs $26.9 \pm 1.1\%$, $p < 0.05$) (Fig. 3D), respectively, than Ex(−).

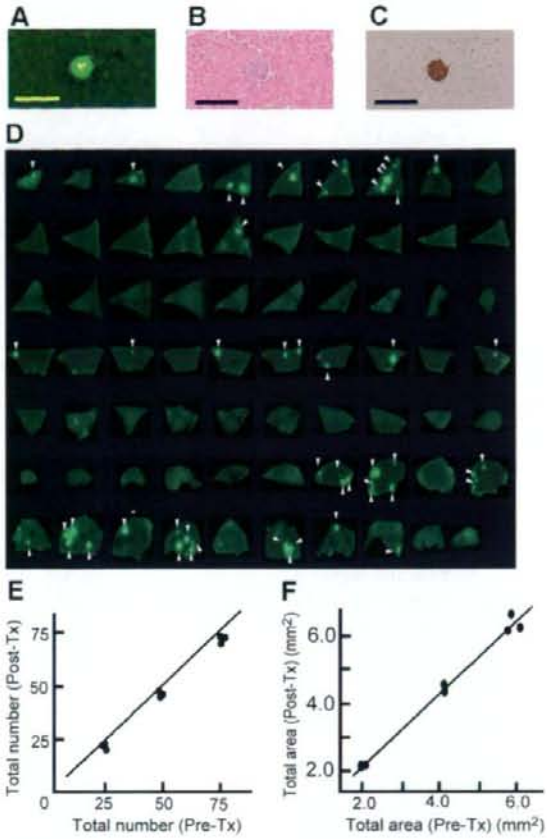

Fig. 2. Islets of transgenic C57BL/6-EGFP mice detected and measured by fluorescence microscopy. (A–C) Photographs of islet grafts in liver. Fluorescent islet (A), HE (B) and insulin immunostaining (C). Scale bar: 200 μm. (D) Representative photographs after transplantation with 50 islets of liver slices under fluorescence microscope. Fluorescent islets are indicated by arrowhead. (E, F) The total number (E) and the total area mass (F) of all EGFP-expressing islets before transplantation compared with fluorescent islet grafts in liver after transplantation ($n = 3$).

Area of islet grafts in liver with and without exendin-4 treatment compared by conventional immunohistochemical analysis

Conventional total area mass measurements, the ratio of the area of islet beta cells to that of the examined liver slice, was compared by immunohistochemical analysis using limited liver sections on Day 1 and Day 3 (Fig. 4A(a and c) and B (e and g)). The conventional relative area mass in Ex(+) was 32.0% and 44.7% higher on Day 1 ($n = 3$ for each, $0.07830 \pm 0.0003\%$ vs $0.0533 \pm 0.0003\%$, $p < 0.05$) and Day 3 ($n = 3$ for each, $0.0680 \pm 0.0009\%$ vs $0.0380 \pm 0.0043\%$, $p < 0.01$) than Ex(−) (Fig. 4C). The ratio of conventional relative area mass of Ex(+) to that of Ex(−) on Day 1 and Day 3 was comparable to the results of measurement of total area mass measured by our novel method.

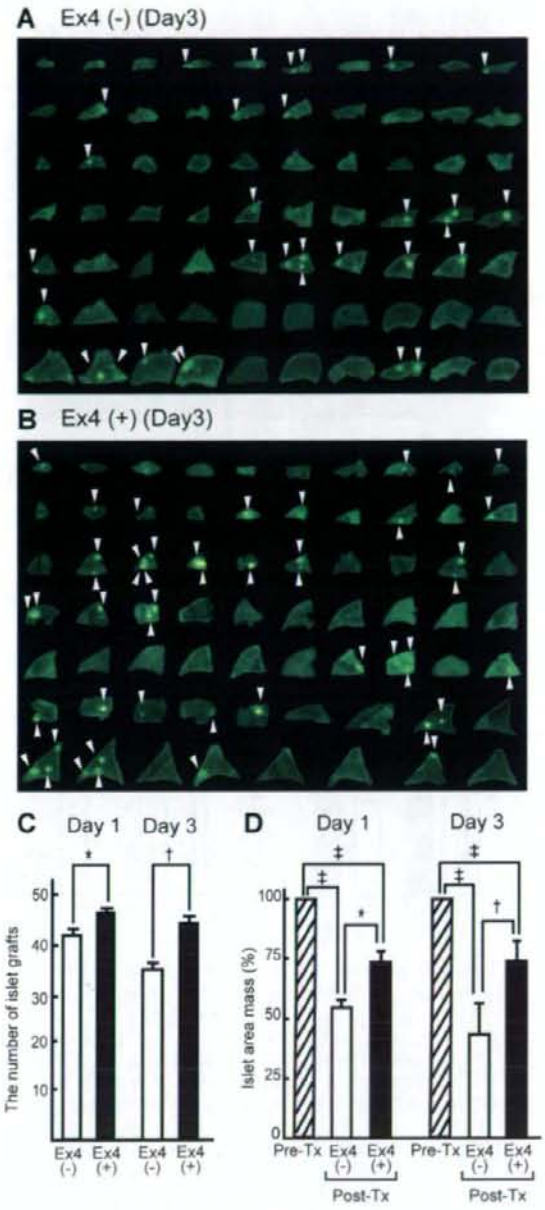

Fig. 3. Exendin-4 preserved transplanted islets during the early posttransplant period in number and total area mass. (A–B) Representative photographs of fluorescent islet grafts in all liver slices from exendin-4-treated mice (Ex4(+)) (A) and -untreated mice (Ex4(−)) (B) on Day 3. (C) Number of islet grafts in liver slices on Day 1 ($n = 3$) and Day 3 ($n = 3$) in Ex4(+) and Ex4(−). $^{*}p < 0.05$ and $^{\dagger}p < 0.01$ vs Ex4(−). (D) Total area mass of all fluorescent islet grafts in liver slices on Day 1 ($n = 3$) and on Day 3 ($n = 3$) in Ex4(+) and Ex(−). Data after transplantation (Post-Tx) and before transplantation (Pre-Tx) are also compared. $^{*}p < 0.05$ and $^{\dagger}p < 0.01$ vs Ex4(−), $^{\ddagger}p < 0.01$ vs Pre-Tx.

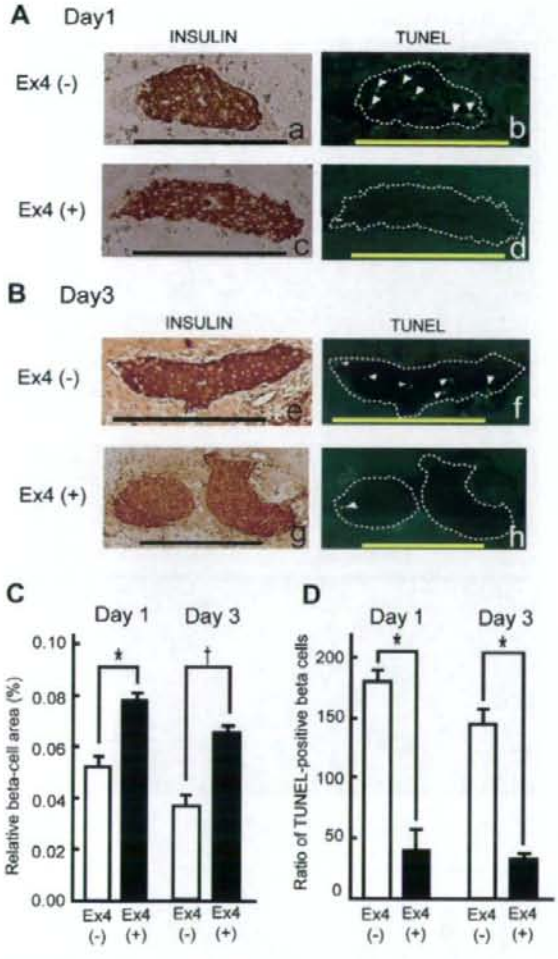

Fig. 4. Exendin-4 treatment reduced beta-cell apoptosis after intraportal islet transplantation. (A–B) Representative photographs of liver sections on Day 1 (A) and Day 3 (B) from Ex4(+) mice and Ex4(−) mice stained for insulin (a, c, e, and g) and TUNEL-assay (b, d, f, and h) are shown. TUNEL-positive cells are indicated by arrowhead. Scale bar: 200 μm. (C) Ex4(+) showed significantly greater beta-cell mass than Ex4(−) on Day 1 ($n = 3$ for each) and Day 3 ($n = 3$ for each). $^{*}p < 0.05$ and $^{\dagger}p < 0.01$ vs Ex4(−). (D) Ex4(+) showed a significantly greater decrease in the ratio of TUNEL-positive beta cells than Ex4(−) on Day 1 ($n = 3$ for each) (number/beta-cell area (mm^2)) and Day 3 ($n = 3$ for each) (number/beta-cell area (mm^2)). $^{*}p < 0.05$ vs Ex4(−).

Exendin-4 decreased the rate of apoptosis of beta cells introduced by intraportal islet graft after transplantation

To investigate the difference in area mass of transplanted islets in Ex(+) and Ex(−), the rate of apoptosis of beta cells of islet grafts on Day 1 and Day 3 was examined (Fig. 4A and B). The rate of apoptosis of TUNEL and insulin-double positive cells was significantly lower on Day 1 ($n = 3$ for each, 246.5 ± 5.5 vs 36.4 ± 3.6 (number/beta-cell area (mm^2)), $p < 0.01$) and on Day 3 ($n = 3$ for each, 148.7 ± 17.7 vs 41.3 ± 1.3 (number/beta-cell area (mm^2)), $p < 0.01$) with Ex(+) than Ex(−) (Fig. 4D).

Discussion

In the present study, we demonstrate that GLP-1R signaling has a cytoprotective effect in the posttransplant period using a murine islet transplantation model. Exendin-4 treatment during the early posttransplant hyperglycemic phase contributed to restore normoglycemia during the late posttransplant phase in STZ-induced diabetic mice receiving a suboptimal graft of 150 islets. In addition, the total number and total area mass of the islet grafts both on Day 1 and Day 3 was significantly greater in Ex(+) than in Ex(−). The finding that the rate of apoptosis was less in Ex(+) than in Ex(−) both on Day 1 and Day 3, when their blood glucose levels were yet unchanged, demonstrates that GLP-1R signaling inhibits apoptosis *in vivo* under conditions of glucose toxicity.

Murine islet transplantation is an ideal model for investigating the cytoprotective effect of exendin-4 on transplanted pancreatic beta cells *in vivo*. Although isogenic islets injected into the portal vein are spared rejection by the immune reaction, the cells may succumb to apoptosis due to various stress factors including hypoxia [18,19], inflammation [20,21], and mechanical shear stress [22,21] before engraftment. The efficacy of exendin-4 treatment on posttransplant hyperglycemic status in this transplantation model can be quantified using different suboptimal numbers of islets because the posttransplant glycemic condition directly reflects the mass of engrafted islets. The number and mass of transplanted islets can be traced because isolated islets can be labeled and examined before transplantation. Thus, this murine islet transplantation model allows observation of the direct effect of the cytoprotective effect on beta cells *in vivo*.

In this study, we established a method for tracing the transplanted islets of transgenic C57BL/6-EGFP mice in liver sections under fluorescence excitation. Our findings reveal that the area of fluorescence of islet grafts in liver coincides with that of insulin immunostaining (Fig. 2A–C), which areas before transplantation correlate highly with those after transplantation (Fig. 2F). Observation of each islet grafts before and after transplantation is definitive for evaluation of the cytoprotective action, which is not practicable by the conventional immunohistochemical method due to the necessarily limited observation of the organ.

We have also shown that the natural course of islet engraftment in the early posttransplant period can involve loss of about half of the transplanted beta cells. Recently, Eich et al. reported evaluation of islet mass by positron-emission tomography using islets labeled with ^{18}Fluorodeoxyglucose, and found that almost 50% of the transplanted islets in the graft were lost [23], which is comparable with our data. Although about 30% of the graft was found to be lost even with exendin-4 treatment on Day 1, the rate

of apoptosis remained lower, resulting in a mass of engraftment more than adequate for normoglycemia thereafter. This finding is encouraging regarding the possible clinical use of exendin-4 in islet transplantation therapy in human subjects [24,25].

Although exendin-4 is already in clinical use for treatment of T2DM [26], this cytoprotective effect on beta cells *in vivo* also certainly functions independently of other actions in T2DM. The mass of islets is usually already decreased when patients are diagnosed with T2DM [27]. Thus, exendin-4 treatment used in the early phase of development, when glycemic tolerance is yet normal, might hamper the progression of T2DM.

Acknowledgments

This work was supported in part by a Scientific Grant and a Grant-in-Aid for Exploratory Research from the Ministry of Education, Culture, Sports, Science, and Technology of Japan, and by Research on Nanotechnical Medicine from the Ministry of Health, Labour, and Welfare of Japan. We thank Dr. M. Okabe for providing us transgenic C57BL/6-EGFP mice.

References

[1] H. Elrick, L. Stimmler, C.J. Hlad Jr., Y. Arai, Plasma insulin response to oral and intravenous glucose administration, J. Clin. Endocrinol. Metab. 24 (1964) 1076–1082.
[2] M.J. Perley, D.M. Kipnis, Plasma insulin responses to oral and intravenous glucose: studies in normal and diabetic subjects, J. Clin. Invest. 46 (1967) 1954–1962.
[3] Y. Li, T. Hansotia, B. Yusta, F. Ris, P.A. Halban, D.J. Drucker, Glucagon-like peptide-1 receptor signaling modulates beta cell apoptosis, J. Biol. Chem. 278 (2003) 471–478.
[4] P.L. Brubaker, D.J. Drucker, Minireview: Glucagon-like peptides regulate cell proliferation and apoptosis in the pancreas, gut, and central nervous system, Endocrinology 145 (2004) 2653–2659.
[5] J.F. List, J.F. Habener, Glucagon-like peptide 1 agonists and the development and growth of pancreatic beta-cells, Am. J. Physiol. Endocrinol. Metab. 286 (2004) E875–E881.
[6] D.J. Drucker, The biology of incretin hormones, Cell Metab. 3 (2006) 153–165.
[7] B. Yusta, L.L. Baggio, J.L. Estall, J.A. Koehler, D.P. Holland, H. Li, D. Pipeleers, Z. Ling, D.J. Drucker, GLP-1 receptor activation improves beta cell function and survival following induction of endoplasmic reticulum stress, Cell Metab. 4 (2006) 391–406.
[8] J. Sun, H. He, B.J. Xie, Novel antioxidant peptides from fermented mushroom Ganoderma lucidum, J. Agric. Food Chem. 52 (2004) 6646–6652.
[9] H. Wang, G. Kouri, C.B. Wollheim, ER stress and SREBP-1 activation are implicated in beta-cell glucolipotoxicity, J. Cell Sci. 118 (2005) 3905–3915.
[10] L.A. Scrocchi, T.J. Brown, N. MaClusky, P.L. Brubaker, A.B. Auerbach, A.L. Joyner, D.J. Drucker, Glucose intolerance but normal satiety in mice with a null mutation in the glucagon-like peptide 1 receptor gene, Nat. Med. 2 (1996) 1254–1258.
[11] A.A. Young, B.R. Gedulin, S. Bhavsar, N. Bodkin, C. Jodka, B. Hansen, M. Denaro, Glucose-lowering and insulin-sensitizing actions of exendin-4: studies in obese diabetic (ob/ob, db/db) mice, diabetic fatty Zucker rats, and diabetic rhesus monkeys (*Macaca mulatta*), Diabetes 48 (1999) 1026–1034.
[12] L. Hansen, C.F. Deacon, C. Orskov, J.J. Holst, Glucagon-like peptide-1-(7–36)amide is transformed to glucagon-like peptide-1-(9–36)amide by dipeptidyl peptidase IV in the capillaries supplying the L cells of the porcine intestine, Endocrinology 140 (1999) 5356–5363.
[13] J.A. Emamaullee, A.M. Shapiro, Factors influencing the loss of beta-cell mass in islet transplantation, Cell Transplant. 16 (2007) 1–8.
[14] M. Okabe, M. Ikawa, K. Kominami, T. Nakanishi, Y. Nishimune, 'Green mice' as a source of ubiquitous green cells, FEBS Lett. 407 (1997) 313–319.
[15] T. Okitsu, S.T. Bartlett, G.A. Hadley, C.B. Drachenberg, A.C. Farney, Recurrent autoimmunity accelerates destruction of minor and major histoincompatible islet grafts in nonobese diabetic (NOD) mice, Am. J. Transplant. 1 (2001) 138–145.
[16] Y. Yonekawa, T. Okitsu, K. Wake, Y. Iwanaga, H. Noguchi, H. Nagata, X. Liu, N. Kobayashi, S. Matsumoto, A new mouse model for intraportal islet transplantation with limited hepatic lobe as a graft site, Transplantation 82 (2006) 712–715.
[17] A. King, J. Lock, G. Xu, S. Bonner-Weir, G.C. Weir, Islet transplantation outcomes in mice are better with fresh islets and exendin-4 treatment, Diabetologia 48 (2005) 2074–2079.
[18] G. Miao, R.P. Ostrowski, J. Mace, J. Hough, A. Hopper, R. Peverini, R. Chinnock, J. Zhang, E. Hathout, Dynamic production of hypoxia-inducible factor-1alpha in early transplanted islets, Am. J. Transplant. 6 (2006) 2636–2643.
[19] M. Giuliani, W. Moritz, E. Bodmer, D. Dindo, P. Kugelmeier, R. Lehmann, M. Gassmann, P. Groscurth, M. Weber, Central necrosis in isolated hypoxic human pancreatic islets: evidence for postisolation ischemia, Cell Transplant. 14 (2005) 67–76.
[20] N.R. Barshes, S. Wyllie, J.A. Goss, Inflammation-mediated dysfunction and apoptosis in pancreatic islet transplantation: implications for intrahepatic grafts, J. Leukoc. Biol. 77 (2005) 587–597.
[21] S. Cabric, J. Sanchez, T. Lundgren, A. Foss, M. Felldin, R. Kallen, K. Salmela, A. Tibell, G. Tufveson, R. Larsson, O. Korsgren, B. Nilsson, Islet surface heparinization prevents the instant blood-mediated inflammatory reaction in islet transplantation, Diabetes 56 (2007) 2008–2015.
[22] J.L. Contreras, C. Eckstein, C.A. Smyth, G. Bilbao, M. Vilatoba, S.E. Ringland, C. Young, J.A. Thompson, J.A. Fernandez, J.H. Griffin, D.E. Eckhoff, Activated protein C preserves functional islet mass after intraportal transplantation: a novel link between endothelial cell activation, thrombosis, inflammation, and islet cell death, Diabetes 53 (2004) 2804–2814.
[23] T. Eich, O. Eriksson, T. Lundgren, Visualization of early engraftment in clinical islet transplantation by positron-emission tomography, N. Engl. J. Med. 356 (2007) 2754–2755.
[24] E.A. Ryan, B.W. Paty, P.A. Senior, D. Bigam, E. Alfadhli, N.M. Kneteman, J.R. Lakey, A.M. Shapiro, Five-year follow-up after clinical islet transplantation, Diabetes 54 (2005) 2060–2069.
[25] K.A. Ghofaili, M. Fung, Z. Ao, M. Meloche, R.J. Shapiro, G.L. Warnock, D. Elahi, G.S. Meneilly, D.M. Thompson, Effect of exenatide on beta cell function after islet transplantation in type 1 diabetes, Transplantation 83 (2007) 24–28.
[26] D.M. Kendall, M.C. Riddle, J. Rosenstock, D. Zhuang, D.D. Kim, M.S. Fineman, A.D. Baron, Effects of exenatide (exendin-4) on glycemic control over 30 weeks in patients with type 2 diabetes treated with metformin and a sulfonylurea, Diabetes Care 28 (2005) 1083–1091.
[27] A.E. Butler, J. Janson, S. Bonner-Weir, R. Ritzel, R.A. Rizza, P.C. Butler, Beta-cell deficit and increased beta-cell apoptosis in humans with type 2 diabetes, Diabetes 52 (2003) 102–110.

available at www.sciencedirect.com

ScienceDirect

journal homepage: www.elsevier.com/locate/diabres

Effect of corosolic acid on gluconeogenesis in rat liver

Kotaro Yamada [a,c], *Masaya Hosokawa* [a,*], *Shimpei Fujimoto* [a], *Hideya Fujiwara* [a], *Yoshihito Fujita* [a], *Norio Harada* [a], *Chizumi Yamada* [a], *Mitsuo Fukushima* [b], *Naoya Ueda* [c], *Tetsuo Kaneko* [d], *Futoshi Matsuyama* [c], *Yuichiro Yamada* [a], *Yutaka Seino* [a,e], *Nobuya Inagaki* [a]

[a] *Department of Diabetes and Clinical Nutrition, Graduate School of Medicine, Kyoto University, 54 Shogoin, Kawahara-cho, Sakyo-ku, Kyoto 606-8507, Japan*
[b] *Department of Health Informatics Research, Translational Research Informatics Center, Foundation for Biomedical Research and Innovation, Kobe, Japan*
[c] *Use Techno Corporation Co. Ltd., Kyoto, Japan*
[d] *Department of Pharmaceutical Science, Hiroshima International University, Hiroshima, Japan*
[e] *Kansai Denryoku Hospital, Osaka, Japan*

ARTICLE INFO

Article history:
Received 2 April 2007
Accepted 21 November 2007
Published on line 4 January 2008

Keywords:
Corosolic acid
Liver
Gluconeogenesis
Fructose-2,6-bisphosphate
cAMP

ABSTRACT

Corosolic acid (CRA), an active component of Banaba leaves (*Lagerstroemia speciosa* L.), decreases blood glucose in diabetic animals and humans. In this study, we investigated the mechanism of action of CRA on gluconeogenesis in rat liver. CRA (20–100 μM) dose-dependently decreased gluconeogenesis in perfused liver and in isolated hepatocytes. Fructose-2,6-bisphosphate (F-2,6-BP), a gluconeogenic intermediate, plays a critical role in hepatic glucose output by regulating gluconeogenesis and glycolysis in the liver. CRA increased the production of F-2,6-BP along with a decrease in intracellular levels of cAMP both in the presence and in the absence of forskolin in isolated hepatocytes. While a cAMP-dependent protein kinase (PKA) inhibitor inhibited hepatic gluconeogenesis, the drug did not intensify the inhibitory effect of CRA on hepatic gluconeogenesis in isolated hepatocytes. These results indicate that CRA inhibits gluconeogenesis by increasing the production of F-2,6-BP by lowering the cAMP level and inhibiting PKA activity in isolated hepatocytes. Furthermore, CRA increased glucokinase activity in isolated hepatocytes without affecting glucose-6-phosphatase activity, suggesting the promotion of glycolysis. These effects on hepatic glucose metabolism may underlie the various anti-diabetic actions of CRA.

1. Introduction

Banaba leaves (*Lagerstroemia speciosa* L.) have been used as a popular traditional medicine in Southeast Asia, and tea made from the leaves has been used to treat diabetes mellitus [1]. The leaves contain large amounts of corosolic acid (CRA) (Fig. 1), which has recently attracted much attention due to its biological activities [2–11]. Miura and co-workers [9,10] suggested that the acute hypoglycemic effect of CRA is derived, at least in part, from an increase in GLUT4 translocation in mouse muscle, and that CRA improves glucose metabolism by reducing insulin resistance. Recently, Fukushima et al. [11] have shown that CRA has lowered post challenge plasma glucose levels in human. However, the

* *Corresponding author.* Tel.: +81 75 751 3560; fax: +81 75 751 4244.
E-mail address: hosokawa@metab.kuhp.kyoto-u.ac.jp (M. Hosokawa).
0168-8227/$ – see front matter © 2007 Elsevier Ireland Ltd. All rights reserved.
doi:10.1016/j.diabres.2007.11.011

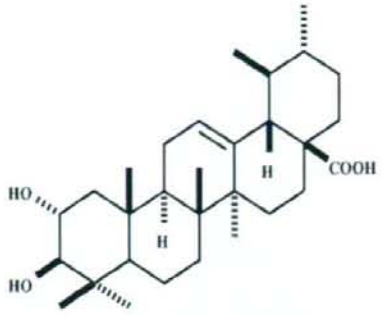

Fig. 1 – Structure of corosolic acid (CRA).

effects of CRA on liver are not well known. The liver is a key regulatory organ of glucose homeostasis, taking up glucose in the fed state and releasing glucose into circulation during starvation, exercise, and when the ratio of insulin to counter-insulin factors is decreased, maintaining blood glucose levels within a narrow physiological range. Impairments in hepatic glucose uptake and production both are characteristic features of the diabetic state [12,13].

In this study, we investigated the acute and direct effects of CRA on hepatic glucose production using perfused liver and isolated hepatocytes to clarify the mechanism of the hypoglycemic effect of CRA.

2. Materials and methods

2.1. *Animals*

Wistar rats were purchased from Shimizu Co., Ltd. (Kyoto, Japan). The rats were allowed access to food and water *ad libitum*, and housed in an air-controlled (temperature 25 ± 2 °C and 50% humidity) room with a 12 h light/dark-cycle. For gluconeogenesis measurements, 7-week-old rats were fasted 24 h with free access to water before the experiment.

2.2. *Materials*

CRA, provided by Use Techno Corporation Co., Ltd. (Kyoto, Japan) was stored at room temperature until use. N-[2-(p-bromocinnamylamino) ethyl]-5-isoquinolinesulfonamide (H89) were from BioMol Co., Ltd. (PA). All enzymes, cofactors, substrates, and chemicals were purchased from Sigma Chemical Co., Ltd. Standard rat chow was from Oriental Yeast Co., Ltd. (Osaka, Japan). [^{14}C]-pyruvate was from American Radiolabeled Chemicals Inc. (St. Louis). All other chemicals were of reagent grade.

2.3. *Gluconeogenesis from lactate in perfused rat liver*

Rat liver perfusion was performed with the flow-through method [14]. The perfused liver system most closely represents physiological conditions. Briefly, Wistar rats were anesthetized with sodium pentobarbital. Krebs-Ringer Buffer (KRB, pH 7.4) containing 1% bovine serum albumin (BSA) without glucose was saturated with 95% O_2/5% CO_2 and maintained at 37 °C. The KRB was infused into the liver through the portal vein with a peristaltic pump at a flow rate of 10 ml/min. CRA was infused into the liver with a syringe pump at a point just before the hepatic portal vein cannula. After 30 min pre-perfusion with the basal KRB, the buffer was replaced with one containing 2 mM lactate as a gluconeogenic precursor. The liver was subsequently perfused with KRB with 2 mM lactate from 30 to 100 min, and the indicated concentration of 20–100 μM CRA was added to KRB with 2 mM lactate from 60 to 80 min. The buffer was then replaced with one without lactate from 100 to 110 min. Samples of effluent perfusion fluid from the caval cannula were collected every 2 min and assayed for glucose. The glucose content was measured by glucose oxidation method (100 Trinder kit, Sigma).

Average glucose output rate during the last 14 min of the 20 min perfusion (66–80 min) [15] with KRB containing 20–100 μM CRA was then measured and compared with control to evaluate the inhibitory effect of CRA.

Liver wet weight was measured at the end of each experiment. CRA was dissolved in dimethylsulfoxide (DMSO), and then diluted with the perfusion buffer at the indicated concentration. The final concentration of DMSO was under 0.1 (v/v)%. In the control studies, the equivalent concentration of DMSO was added to KRB.

2.4. *Isolation of rat hepatocytes*

Twenty-four hour-starved liver of 7-week-old rats was perfused through the inferior *vena cava* with a buffer consisting of 140 mM NaCl, 2.6 mM KCl, 0.28 mM Na_2HPO_4, 5 mM glucose, and 10 mM Hepes (pH 7.4), after pentobarbital sodium anesthesia as described previously [16]. The perfusion was first for 5 min with the buffer supplemented with 0.1 mM EGTA and then for 15 min with the buffer containing 5 mM $CaCl_2$ and 0.2 mg/ml collagenase type 2 (Worthington, Lakewood, NJ). All of the solutions were prewarmed at 37 °C and gassed with a mixture of 95% O_2/5%CO_2, resulting in pH 7.4. The isolated hepatocytes were filtered with nylon mesh (0.75 mm in diameter) and washed twice with the buffer above without collagenase, suspended in a small volume of DMEM (GIBCO, Rockville, MD) without glucose or lactate or pyruvate, and counted. Hepatocyte viability was over 90%, determined by the trypan blue-exclusion method.

2.5. *Gluconeogenesis from lactate in isolated rat hepatocyte*

For gluconeogenesis measurements, isolated hepatocytes were incubated at 37 °C in a humidified atmosphere (5% CO_2) of DMEM without glucose but containing 1 mM lactate and 0.24 mM 3-isobutyl-1-methylxanthine (IBMX) in the presence of CRA or vehicle for 20 min. CRA was dissolved in DMSO, to a concentration in the medium that did not interfere with cell viability (maximally 0.1%, v/v). Incubation was stopped by placing the cells on ice, followed by centrifugation at 4 °C for 1 min at 600 × *g*. The supernatant was removed, the cells were lysed in 0.1% of SDS in phosphate buffered saline (PBS), and the protein content was measured with a

commercially available Protein Assay kit (Bio-Rad, Hercules, CA). The glucose content of the supernatant was measured by glucose oxidation method (100 Trinder kit, Sigma).

2.6. Biosynthetic labeling

Isolated hepatocytes were incubated at 37 °C in a humidified atmosphere (5% CO_2) in 0.5 ml of DMEM with 10 mM glucose, 1 mM pyruvate, and 0.24 mM IBMX, and 0.05 μCi of [^{14}C]-pyruvate in the presence of CRA or vehicle for 20 min. Incubation was stopped by placing the cells on ice, followed by centrifugation at 4 °C for 1 min at 600 × *g*. The supernatant including neosynthesized [^{14}C]-glucose was removed. The cells were lysed in 0.1% of SDS in PBS and the protein content was measured as described above.

2.7. [^{14}C]-glucose measurement and analysis

Neosynthesized [^{14}C]-glucose was separated from charged metabolites by passage of the supernatants mentioned above on anion and cation exchangers (Dowex AG1-X8 and 50W-X8, respectively; Bio-Rad, Hercules, CA) as described [16]. Radioactivity was determined by liquid scintillation counting on a Liquid Scintillation Analyzer (model TRI-CABB 1900CA, Packard Instrument Company Inc., Downers Grove, IL).

2.8. Fructose-2,6-bisphosphate (F-2,6-BP) content in isolated hepatocytes

Isolated hepatocytes were treated at 37 °C in a humidified atmosphere (5% CO_2) of DMEM with or without 10 mM glucose but containing 1 mM lactate, 0.24 mM IBMX in the presence of CRA or vehicle for 20 min. F-2,6-BP was extracted from the hepatocytes in NaOH and kept at 80 °C for 5 min. The extract was collected and neutralized at 0 °C by addition of ice-cold 1 M acetic acid in the presence of 20 mM HEPES. After centrifugation at 8,000 × *g* for 10 min, supernatant was collected and assayed for F-2,6-BP by the 6-phosphofructo-1-kinase (PFK-1) activation method [17] and expressed as nmol/mg protein.

2.9. Determination of cAMP level in isolated hepatocytes

Isolated hepatocytes were treated at 37 °C in a humidified atmosphere (5% CO_2) of DMEM not containing glucose but with or without 5 μM forskolin and with 1 mM lactate and 0.24 mM IBMX in the presence of CRA or vehicle for 20 min. The cell culture medium was removed and the cells were lysed by addition of 0.1 N HCl. The solutions were incubated at 4 °C for 15 min with gentle rotation. The samples were centrifuged for 10 min at 600 × *g*. Aliquots were stocked at −80 °C. The cAMP level in hepatocytes was determined with a commercially available kit (R & D Systems, MN) and expressed as pmol/mg protein.

2.10. Measurement of glucokinase (GK) and hexokinase (HK) activity

Isolated hepatocytes were treated at 37 °C in a humidified atmosphere (5% CO_2) of DMEM without glucose but containing 1 mM lactate, 0.24 mM IBMX in the presence of CRA or vehicle for 20 min. Incubation was stopped by placing the cells on ice, followed by centrifugation at 4 °C for 1 min at 600 × *g*. GK activity was measured by a fluorometric assay according to a method reported previously [18]. The supernatant was removed and the cells were homogenized with a Teflon–glass homogenizer in 3 vol.% of 100 mM Hepes-NaOH buffer (pH 7.6) containing 100 mM KCl, 2 mM $MgCl_2$, 1 mM EDTA, 1 mM DTT, and 2 mg/l leupeptin, and centrifuged for 1 h at 20,000 × *g* at 4 °C. The glucose phosphorylation rate was estimated by the increase in NADH through the following reaction: glucose-6-phosphate + NAD → 6-phospho-glucono-σ lactone + NADH-dependent glucose-6-phosphate dehydrogenase (G6PDH). The enzyme reaction was performed using 25 μl of hepatocyte extracts in a 160 μl solution consisting of 100 mM Tris–HCl buffer (pH 8.0) containing 100 mM KCl, 8 mM $MgCl_2$, 5 mM ATP, 0.5 mM NAD, 1 mM DTT, 0.1 g/l BSA, 1 U/ml G6PDH supplement with two concentrations (50 and 0.5 mM) of glucose at 37 °C for 1 h. The reaction was stopped by adding 290 μl of stopping solution (300 mM Na_2HPO_4, 0.46 mM SDS, pH 8.0). NADH concentration was measured by fluorometry (Shimazu RF-5000, Kyoto, Japan) at 340 nm excitation and 450 nm emission. Blanks in the absence of ATP were incubated in a parallel experiment and subtracted from the total fluorescence of the corresponding complete reaction mixtures. The reaction mixture was pre-incubated for 3 min and the reaction was started by the addition of ATP. GK activity was determined by subtracting HK activity measured at 0.5 mM glucose from the activity measured at 50 mM glucose. Enzyme activities are expressed as the number of substrate molecules converted by 1 mg cytosolic protein per minute.

2.11. Measurement of glucose-6- phosphatase (G6Pase) activity

Isolated hepatocytes were treated at 37 °C in a humidified atmosphere (5% CO_2) of DMEM without glucose but containing 1 mM lactate, 0.24 mM IBMX in the presence of CRA or vehicle for 20 min. Incubation was stopped by placing the cells on ice, followed by centrifugation at 4 °C for 1 min at 600 × *g*. The supernatant was removed and the cells were homogenized with a Teflon–glass homogenizer. In the microsomal preparation for the G6Pase assay, 50 mM Tris–HCl, pH 7.5, containing 250 mM sucrose and 0.2 mM EDTA, was used as the homogenizing buffer [19]. For assay of G6Pase, liver microsomal fraction was prepared as follows: homogenate obtained as above was centrifuged at 20,000 × *g* for 20 min at 4 °C, and the 20,000 × *g* supernatant was ultracentrifuged at 105,000 × *g* for 1 h at 4 °C. The resulting sediments were used for G6Pase assay [19]. G6Pase activity was measured with intact microsomal preparation, and determined as described by Passonneau and Lowry [20]. Enzyme activities are expressed as the number of substrate molecules converted by 1 mg microsomal protein per minute.

2.12. Statistical analysis

Significant difference was determined using one-factor ANOVA followed by *t*-test. *P* values of <0.05 were considered